Appl. Math. Mech. -Engl. Ed., **43**(2), 167–184 (2022)

APPLIED MATHEMATICS AND MECHANICS (ENGLISH EDITION)

https://doi.org/10.1007/s10483-021-2808-9

Tunable three-dimensional nonreciprocal transmission in a layered nonlinear elastic wave metamaterial by initial stresses*

Zhenni LI[1], Yize WANG[2,†], Yuesheng WANG[1,2,†]

1. Institute of Engineering Mechanics, Beijing Jiaotong University, Beijing 100044, China;
2. Department of Mechanics, Tianjin University, Tianjin 300350, China

(Received Mar. 5, 2021 / Revised Nov. 15, 2021)

Abstract In this work, the three-dimensional (3D) propagation behaviors in the nonlinear phononic crystal and elastic wave metamaterial with initial stresses are investigated. The analytical solutions of the fundamental wave and second harmonic with the quasi-longitudinal (qP) and quasi-shear (qS_1 and qS_2) modes are derived. Based on the transfer and stiffness matrices, band gaps with initial stresses are obtained by the Bloch theorem. The transmission coefficients are calculated to support the band gap property, and the tunability of the nonreciprocal transmission by the initial stress is discussed. This work is expected to provide a way to tune the nonreciprocal transmission with vector characteristics.

Key words nonlinear elastic wave metamaterial, nonreciprocal transmission, three-dimensional (3D) elastic wave, initial stress

Chinese Library Classification O343.5
2010 Mathematics Subject Classification 74J30

1 Introduction

Phononic crystals consist of two or more materials periodically, and can generate band gap of elastic waves[1–5]. Band gaps are certain frequency regions in which the elastic wave propagation is prohibited[6–7]. Elastic wave metamaterial is a new concept proposed in recent years, which brings extraordinary phenomena[8–15]. These periodic structures have the ability to control the wave propagation and vibration, which results in some advanced devices in practice.

The material nonlinearity can illustrate interesting wave phenomena and transmission behaviors, which has attracted considerable attention[16–20]. The distinguishing property of the material nonlinearity is the generation of higher-order harmonic. Liang et al.[21–22] studied an acoustic diode consisting of a linear phononic crystal and a nonlinear layer to show the nonreciprocal transmission of the acoustic wave. The nonreciprocal transmission means that waves can propagate in one direction but are prohibited in the reverse. Recently, increasing attention

* Citation: LI, Z. N., WANG, Y. Z., and WANG, Y. S. Tunable three-dimensional nonreciprocal transmission in a layered nonlinear elastic wave metamaterial by initial stresses. *Applied Mathematics and Mechanics* (*English Edition*), **43**(2), 167–184 (2022) https://doi.org/10.1007/s10483-021-2808-9

† Corresponding authors, E-mails: wangyize@tju.edu.cn; yswang@tju.edu.cn

Project supported by the National Natural Science Foundation of China (Nos. 11922209, 11991031, and 12021002)

has been paid to the phenomenon in which the reciprocity theorem of the classic wave system is broken[23–30].

However, the above-mentioned studies mainly focused on scalar waves with only one displacement component. In recent years, the propagation of three-dimensional (3D) harmonic waves in layered structures have been reported[31–34]. In our previous work, the nonreciprocal transmission in 3D cases in a layered nonlinear elastic wave metamaterial was discussed[35]. Moreover, some studies have indicated that the effects of the external initial stresses on the band gap are significant[36–38]. As a result, the initial stress can offer a new opportunity to tune the 3D nonreciprocal transmission.

In this investigation, the nonreciprocal transmission of 3D waves in a layered nonlinear elastic wave metamaterial with initial stresses is studied. Combining the band gap in the linear phononic crystal and material nonlinearity breaks the reciprocity theorem of elastic waves. According to the transfer and stiffness matrices, the band gaps and transmission coefficients of the fundamental wave and the second harmonic are obtained. The effects of the initial stresses on propagation behaviors are discussed.

2 Governing equation with initial stresses

Figure 1(a) shows a one-dimensional (1D) nonlinear phononic crystal with initial stresses and the local coordinate of each sub-cell. This structure is formed by two different nonlinear materials A and B, which consists of m unit cells. d_1 and d_2 denote the widths of the layers A and B, respectively, and the thickness of a unit cell is $d = d_1 + d_2$. The characters $2n-1$, $2n$, and $2n+1$ indicate the interfaces of the nth unit cell. The normal initial stresses σ^0_{11}, σ^0_{22}, and σ^0_{33} are taken into account. For an incident elastic wave in the 3D space, the propagation direction is denoted by the polar and azimuthal angles θ_1 and θ_2.

As shown in Fig. 1(b), a nonlinear elastic wave metamaterial is composed of a 1D phononic crystal with layers of linear materials C and D and a nonlinear medium A. We assume that the elastic wave from the right to the left is the positive direction, and the reverse case represents the negative one. The nonreciprocal transmission can be obtained by the combination of the linearly periodic structure and nonlinear material. Then, the elastic wave can propagate in the positive direction but stop in the negative one, which shows the diode characteristic of the elastic wave.

For the 3D elastic wave propagation, the displacement components with time t can be

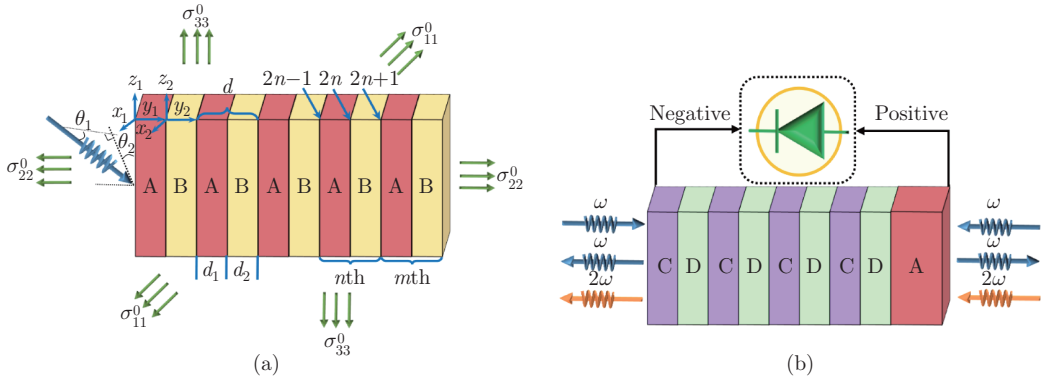

Fig. 1 Layered nonlinear phononic crystal and elastic wave metamaterial with initial stresses (color online)

written as

$$u_i = u_i(x, y, z, t). \tag{1}$$

The governing equation of the anisotropic monoclinic medium with initial stresses can be expressed as[31,39]

$$\sigma_{ij,j} + (\sigma^0_{kj} w_{ik} + \sigma^0_{ij}\varepsilon_{ll} - \sigma^0_{ik}\varepsilon_{kj}) = \rho u_{i,tt}, \quad i, j, k, l = x, y, z, \tag{2}$$

where ρ is the mass density, the commas in the subscripts refer to the derivative with respect to the time or space coordinates, and

$$w_{ik} = \frac{u_{i,k} - u_{k,i}}{2}, \quad \varepsilon_{ll} = u_{l,l}, \quad \varepsilon_{kj} = \frac{u_{k,j} + u_{j,k}}{2}. \tag{3}$$

The constitutive equation with material nonlinearity can be written as[40]

$$\sigma_{ij} = c_{ijkl} u_{k,l} + \frac{1}{2} m_{ijklmn} u_{k,l} u_{m,n}, \tag{4}$$

where $m_{ijklmn} = c_{ijklmn} + c_{ijln}\delta_{km} + c_{jnkl}\delta_{im} + c_{jlmn}\delta_{ik}$, in which c_{ijklmn} is the third-order elastic constant, c_{ijkl}, c_{ijln}, c_{jnkl}, and c_{jlmn} denote the second-order constants, δ_{km}, δ_{im}, and δ_{ik} represent the Kronecker delta, and u_k and u_m are the mechanical displacements.

The displacement components can be expressed as

$$u_i = u_i^{(1)} + u_i^{(2)}, \tag{5}$$

where $u_i^{(1)}$ and $u_i^{(2)}$ denote the displacement components of the fundamental wave and the second harmonic, respectively.

Based on the perturbation approximation method, the governing equations with initial stresses of the fundamental wave and the second harmonic can be derived as

$$\begin{aligned}
&\rho_p u^{(1)}_{px,tt} - C_{p11} u^{(1)}_{px,xx} - 2C_{p15} u^{(1)}_{px,xz} - (C_{p66} + (\sigma^0_{22}/2) - (\sigma^0_{11}/2)) u^{(1)}_{px,yy} - (C_{p55} + (\sigma^0_{33}/2) \\
&- (\sigma^0_{11}/2)) u^{(1)}_{px,zz} - (C_{p12} + C_{p66} + (\sigma^0_{11}/2) - (\sigma^0_{22}/2)) u^{(1)}_{py,xy} - (C_{p46} + C_{p25}) u^{(1)}_{py,yz} \\
&- C_{p15} u^{(1)}_{pz,xx} - (C_{p13} + C_{p55} + (\sigma^0_{11}/2) - (\sigma^0_{33}/2)) u^{(1)}_{pz,xz} - C_{p46} u^{(1)}_{pz,yy} - C_{p35} u^{(1)}_{pz,zz} = 0,
\end{aligned} \tag{6a}$$

$$\begin{aligned}
&\rho_p u^{(1)}_{py,tt} - (C_{p66} + C_{p12} + (\sigma^0_{22}/2) - (\sigma^0_{11}/2)) u^{(1)}_{px,xy} - (C_{p25} + C_{p46}) u^{(1)}_{px,yz} - (C_{p66} + (\sigma^0_{11}/2) \\
&- (\sigma^0_{22}/2)) u^{(1)}_{py,zz} - 2C_{p46} u^{(1)}_{py,xz} - C_{p22} u^{(1)}_{py,yy} - (C_{p44} + (\sigma^0_{33}/2) - (\sigma^0_{22}/2)) u^{(1)}_{py,zz} \\
&- (C_{p46} + C_{p25}) u^{(1)}_{pz,xy} - (C_{p23} + C_{p44} + (\sigma^0_{22}/2) - (\sigma^0_{33}/2)) u^{(1)}_{pz,yz} = 0,
\end{aligned} \tag{6b}$$

$$\begin{aligned}
&\rho_p u^{(1)}_{pz,tt} - C_{p15} u^{(1)}_{px,xx} - (C_{p55} + C_{p13} + (\sigma^0_{33}/2) - (\sigma^0_{11}/2)) u^{(1)}_{px,xz} - C_{p46} u^{(1)}_{px,yy} - C_{p35} u^{(1)}_{px,zz} \\
&- (C_{p25} + C_{p46}) u^{(1)}_{py,xy} - (C_{p44} + C_{p23} + (\sigma^0_{33}/2) - (\sigma^0_{22}/2)) u^{(1)}_{py,yz} - (C_{p55} + (\sigma^0_{11}/2) \\
&- (\sigma^0_{33}/2)) u^{(1)}_{pz,xx} - 2C_{p35} u^{(1)}_{pz,xz} - (C_{p44} + (\sigma^0_{22}/2) - (\sigma^0_{33}/2)) u^{(1)}_{pz,yy} - C_{p33} u^{(1)}_{pz,zz} = 0,
\end{aligned} \tag{6c}$$

$$\begin{aligned}
&\rho_p u^{(2)}_{px,tt} - C_{p11} u^{(2)}_{px,xx} - 2C_{p15} u^{(2)}_{px,xz} - (C_{p66} + (\sigma^0_{22}/2) - (\sigma^0_{11}/2)) u^{(2)}_{px,yy} - (C_{p55} + (\sigma^0_{33}/2) \\
&- (\sigma^0_{11}/2)) u^{(2)}_{px,zz} - (C_{p12} + C_{p66} + (\sigma^0_{11}/2) - (\sigma^0_{22}/2)) u^{(2)}_{py,xy} - (C_{p46} + C_{p25}) u^{(2)}_{py,yz} \\
&- C_{p15} u^{(2)}_{pz,xx} - (C_{p13} + C_{p55} + (\sigma^0_{11}/2) - (\sigma^0_{33}/2)) u^{(2)}_{pz,xz} - C_{p46} u^{(2)}_{pz,yy} - C_{p35} u^{(2)}_{pz,zz} \\
&= F_1(u_p^{(1)}),
\end{aligned} \tag{6d}$$

$$\begin{aligned}
&\rho_p u^{(2)}_{py,tt} - (C_{p66} + C_{p12} + (\sigma^0_{22}/2) - (\sigma^0_{11}/2)) u^{(2)}_{px,xy} - (C_{p25} + C_{p46}) u^{(2)}_{px,yz} - (C_{p66} + (\sigma^0_{11}/2) \\
&- (\sigma^0_{22}/2)) u^{(2)}_{py,zz} - 2C_{p46} u^{(2)}_{py,xz} - C_{p22} u^{(2)}_{py,yy} - (C_{p44} + (\sigma^0_{33}/2) - (\sigma^0_{22}/2)) u^{(2)}_{py,zz} \\
&- (C_{p46} + C_{p25}) u^{(2)}_{pz,xy} - (C_{p23} + C_{p44} + (\sigma^0_{22}/2) - (\sigma^0_{33}/2)) u^{(2)}_{pz,yz} = F_2(u_p^{(1)}),
\end{aligned} \tag{6e}$$

$$\begin{aligned}&\rho_p u^{(2)}_{pz,tt} - C_{p15}u^{(2)}_{px,xx} - (C_{p55} + C_{p13} + (\sigma^0_{33}/2) - (\sigma^0_{11}/2))u^{(2)}_{px,xz} - C_{p46}u^{(2)}_{px,yy} - C_{p35}u^{(2)}_{px,zz}\\&- (C_{p25} + C_{p46})u^{(2)}_{py,xy} - (C_{p44} + C_{p23} + (\sigma^0_{33}/2) - (\sigma^0_{22}/2))u^{(2)}_{py,yz} - (C_{p55} + (\sigma^0_{11}/2)\\&- (\sigma^0_{33}/2))u^{(2)}_{pz,xx} - 2C_{p35}u^{(2)}_{pz,xz} - (C_{p44} + (\sigma^0_{22}/2) - (\sigma^0_{33}/2))u^{(2)}_{pz,yy} - C_{p33}u^{(2)}_{pz,zz}\\&= F_3(u^{(1)}_p),\end{aligned} \tag{6f}$$

where the subscript $p\,(p = 1, 2)$ refers to the material of each sub-cell, $u^{(1)}_{pi}$ and $u^{(2)}_{pi}$ are the displacement components of the fundamental wave and the second harmonic, respectively, C_{pmn} $(m, n = 1, 2, \cdots, 6)$ represent the second-order elastic constants, and $F_i(u^{(1)}_p)$ is the bulk driving force of the second harmonic generated by the interaction between the fundamental wave and material nonlinearity[16,41]. The explicit expressions of $F_i(u^{(1)}_p)$ can be found in Ref. [35] and are not presented here for simplicity.

From Eqs. (6a)–(6c), we can see that the displacements of the fundamental wave along three directions are coupled. Accordingly, the analytical solutions depending on x_p, y_p, and z_p can be given as

$$(u^{(1)}_{px}, u^{(1)}_{py}, u^{(1)}_{pz}) = (U^{(1)}_{px}, U^{(1)}_{py}, U^{(1)}_{pz}) \exp\Big(\frac{\mathrm{i}\omega}{c^{(1)}}(q_{p1}x_p + \alpha_p y_p + q_{p2}z_p - c^{(1)}t)\Big), \tag{7}$$

where $U^{(1)}_{px}$, $U^{(1)}_{py}$, and $U^{(1)}_{pz}$ are the displacement amplitudes, $q_{p1} = \sin\theta_1\cos\theta_2$, $q_{p2} = \sin\theta_1\sin\theta_2$, $c^{(1)} = \omega/k^{(1)}$ is the phase velocity of the incident fundamental wave, ω and $k^{(1)}$ denote the frequency and the wave number, respectively, and $\mathrm{i} = \sqrt{-1}$.

Substituting Eq. (7) into Eqs. (6a)–(6c) yields

$$\begin{pmatrix} T_{p11} & T_{p12} & T_{p13} \\ T_{p21} & T_{p22} & T_{p23} \\ T_{p31} & T_{p32} & T_{p33} \end{pmatrix} \begin{pmatrix} U^{(1)}_{px} \\ U^{(1)}_{py} \\ U^{(1)}_{pz} \end{pmatrix} = \begin{pmatrix} 0 \\ 0 \\ 0 \end{pmatrix}, \tag{8}$$

where

$$\begin{aligned}T_{p11} &= C_{p11}q^2_{p1} + 2C_{p15}q_{p1}q_{p2} + C_{p66}\alpha^2_p + C_{p55}q^2_{p2} + \frac{\sigma^0_{22} - \sigma^0_{11}}{2}\alpha^2_p\\&\quad + \frac{\sigma^0_{33} - \sigma^0_{11}}{2}q^2_{p2} - \rho_p(c^{(1)})^2,\end{aligned} \tag{9a}$$

$$T_{p12} = C_{p12}q_{p1}\alpha_p + C_{p46}q_{p2}\alpha_p + C_{p66}q_{p1}\alpha_p + C_{p25}q_{p2}\alpha_p + \frac{\sigma^0_{11} - \sigma^0_{22}}{2}q_{p1}\alpha_p, \tag{9b}$$

$$T_{p13} = C_{p13}q_{p1}q_{p2} + C_{p15}q^2_{p1} + C_{p46}\alpha^2_p + C_{p35}q^2_{p2} + C_{p55}q_{p1}q_{p2} + \frac{\sigma^0_{11} - \sigma^0_{33}}{2}q_{p1}q_{p2}, \tag{9c}$$

$$T_{p21} = C_{p12}q_{p1}\alpha_p + C_{p46}q_{p2}\alpha_p + C_{p66}q_{p1}\alpha_p + C_{p25}q_{p2}\alpha_p + \frac{\sigma^0_{22} - \sigma^0_{11}}{2}q_{p1}\alpha_p, \tag{9d}$$

$$\begin{aligned}T_{p22} &= 2C_{p46}q_{p1}q_{p2} + C_{p66}q^2_{p1} + C_{p22}\alpha^2_p + C_{p44}q^2_{p2} + \frac{\sigma^0_{11} - \sigma^0_{22}}{2}q^2_{p1}\\&\quad + \frac{\sigma^0_{33} - \sigma^0_{22}}{2}q^2_{p2} - \rho_p(c^{(1)})^2,\end{aligned} \tag{9e}$$

$$T_{p23} = C_{p46}q_{p1}\alpha_p + C_{p23}q_{p2}\alpha_p + C_{p25}q_{p1}\alpha_p + C_{p44}q_{p2}\alpha_p + \frac{\sigma^0_{22} - \sigma^0_{33}}{2}q_{p2}\alpha_p, \tag{9f}$$

$$T_{p31} = C_{p13}q_{p1}q_{p2} + C_{p15}q^2_{p1} + C_{p46}\alpha^2_p + C_{p35}q^2_{p2} + C_{p55}q_{p1}q_{p2} + \frac{\sigma^0_{33} - \sigma^0_{11}}{2}q_{p1}q_{p2}, \tag{9g}$$

$$T_{p32} = C_{p46}q_{p1}\alpha_p + C_{p23}q_{p2}\alpha_p + C_{p25}q_{p1}\alpha_p + C_{p44}q_{p2}\alpha_p + \frac{\sigma^0_{33} - \sigma^0_{22}}{2}q_{p2}\alpha_p, \tag{9h}$$

$$T_{p33} = 2C_{p35}q_{p1}q_{p2} + C_{p55}q^2_{p1} + C_{p44}\alpha^2_p + \frac{\sigma^0_{11} - \sigma^0_{33}}{2}q^2_{p1} + \frac{\sigma^0_{22} - \sigma^0_{33}}{2}\alpha^2_p - \rho_p(c^{(1)})^2. \tag{9i}$$

The existence of non-trivial solutions in Eq. (8) requires the coefficient determinant being zero. Then, the characteristic equation can be derived as

$$A_6\alpha_p^6 + A_4\alpha_p^4 + A_2\alpha_p^2 + A_0 = 0, \tag{10}$$

where the expressions of A_6, A_4, A_2, and A_0 are presented in Appendix A.

Then, three pairs of conjugative roots can be obtained by the sixth-order polynomial, which denote the coupled quasi-shear (qS_2 and qS_1) and quasi-longitudinal (qP) waves. We assume that α_{p1}, α_{p3}, and α_{p5} represent the transmitted qS_2, qS_1, and qP waves, while α_{p2}, α_{p4}, and α_{p6} mean the reflected qS_2, qS_1, and qP ones.

We define the amplitude ratios for the coupled waves as

$$a_{p2}^{(1)} = \frac{U_{py}^{(1)}}{U_{px}^{(1)}} = \frac{T_{p13}T_{p21} - T_{p11}T_{p23}}{T_{p12}T_{p23} - T_{p13}T_{p22}}, \tag{11a}$$

$$a_{p3}^{(1)} = \frac{U_{pz}^{(1)}}{U_{px}^{(1)}} = \frac{T_{p11}T_{p22} - T_{p12}T_{p21}}{T_{p12}T_{p23} - T_{p13}T_{p22}}. \tag{11b}$$

The term $\exp(-\mathrm{i}\omega t)$ is ignored in the following derivation for simplicity. Then, the displacement and stress components of the coupled waves can be expressed as

$$(u_{pxq}^{(1)}, u_{pyq}^{(1)}, u_{pzq}^{(1)}) = (1, a_{p2q}^{(1)}, a_{p3q}^{(1)})U_{pxq}^{(1)} \exp\Big(\frac{\mathrm{i}\omega}{c^{(1)}}(q_{p1}x_p + \alpha_{pq}y_p + q_{p2}z_p)\Big), \tag{12a}$$

$$(\sigma_{p12q}^{(1)}, \sigma_{p22q}^{(1)}, \sigma_{p23q}^{(1)}) = \frac{\mathrm{i}\omega}{c^{(1)}}(G_{p1q}^{(1)}, G_{p2q}^{(1)}, G_{p3q}^{(1)})U_{pxq}^{(1)} \exp\Big(\frac{\mathrm{i}\omega}{c^{(1)}}(q_{p1}x_p + \alpha_{pq}y_p + q_{p2}z_p)\Big), \tag{12b}$$

where $q = 1, 2, \cdots, 6$, and

$$G_{p1q}^{(1)} = C_{p46}q_{p2}a_{p2q}^{(1)} + C_{p46}\alpha_{pq}a_{p3q}^{(1)} + C_{p66}\alpha_{pq} + C_{p66}q_{p1}a_{p2q}^{(1)} - \frac{\sigma_{11}^0 + \sigma_{22}^0}{2}q_{p1}a_{p2q}^{(1)}, \tag{13a}$$

$$\begin{aligned} G_{p2q}^{(1)} =& C_{p12}q_{p1} + C_{p22}\alpha_{pq}a_{p2q}^{(1)} + C_{p23}q_{p2}a_{p3q}^{(1)} + C_{p25}q_{p2} + C_{p25}q_{p1}a_{p3q}^{(1)} \\ &+ \sigma_{22}^0(q_{p1} + q_{p2}a_{p3q}^{(1)}), \end{aligned} \tag{13b}$$

$$G_{p3q}^{(1)} = C_{p44}q_{p2}a_{p2q}^{(1)} + C_{p44}\alpha_{pq}a_{p3q}^{(1)} + C_{p46}\alpha_{pq} + C_{p46}q_{p1}a_{p2q}^{(1)} - \frac{\sigma_{22}^0 + \sigma_{33}^0}{2}q_{p2}a_{p2q}^{(1)}. \tag{13c}$$

The fundamental wave in each nonlinear layer can generate the bulk driving force for the second harmonic as

$$\begin{aligned} F_i(u_p^{(1)}) =& \sum_{m=1,2}^{n=3,4,5,6} U_{pi(c_m-c_n)}^{\mathrm{DL}} \exp\Big(\frac{\mathrm{i}\omega}{c^{(1)}}(\alpha_{pm} + \alpha_{pn})y_p + \frac{2\mathrm{i}\omega}{c^{(1)}}(q_{p1}x_p + q_{p2}z_p)\Big) \\ &+ \sum_{m=1,2}^{n=3,4,5,6} U_{pi(c_m-c_n)}^{\mathrm{DT}} \exp\Big(\frac{\mathrm{i}\omega}{c^{(1)}}(\alpha_{pm} + \alpha_{pn})y_p + \frac{2\mathrm{i}\omega}{c^{(1)}}(q_{p1}x_p + q_{p2}z_p)\Big) \\ &+ \sum_{l=3,4}^{h=5,6} U_{pi(c_l-c_h)}^{\mathrm{DL}} \exp\Big(\frac{\mathrm{i}\omega}{c^{(1)}}(\alpha_{pl} + \alpha_{ph})y_p + \frac{2\mathrm{i}\omega}{c^{(1)}}(q_{p1}x_p + q_{p2}z_p)\Big) \\ &+ \sum_{l=3,4}^{h=5,6} U_{pi(c_l-c_h)}^{\mathrm{DT}} \exp\Big(\frac{\mathrm{i}\omega}{c^{(1)}}(\alpha_{pl} + \alpha_{ph})y_p + \frac{2\mathrm{i}\omega}{c^{(1)}}(q_{p1}x_p + q_{p2}z_p)\Big) \\ &+ \sum_{q=1}^{6} U_{pi(c_q-c_q)}^{\mathrm{DL}} \exp\Big(\frac{2\mathrm{i}\omega}{c^{(1)}}(q_{p1}x_p + \alpha_{pq}y_p + q_{p2}z_p)\Big) \\ &+ (U_{pi(c_1-c_2)}^{\mathrm{DL}} + U_{pi(c_3-c_4)}^{\mathrm{DL}} + U_{pi(c_5-c_6)}^{\mathrm{DL}}) \exp\Big(\frac{2\mathrm{i}\omega}{c^{(1)}}(q_{p1}x_p + q_{p2}z_p)\Big), \end{aligned} \tag{14}$$

where $U^{\mathrm{DL}}_{pi(c_m-c_n)}$, $U^{\mathrm{DT}}_{pi(c_m-c_n)}$, $U^{\mathrm{DL}}_{pi(c_l-c_h)}$, $U^{\mathrm{DT}}_{pi(c_l-c_h)}$, $U^{\mathrm{DL}}_{pi(c_q-c_q)}$, $U^{\mathrm{DL}}_{pi(c_1-c_2)}$, $U^{\mathrm{DL}}_{pi(c_3-c_4)}$, and $U^{\mathrm{DL}}_{pi(c_5-c_6)}$ are amplitudes of the bulk driving force. The superscripts DL and DT mean the components of the driving force with longitudinal and transverse waves, respectively.

The displacement components of the second harmonic can be derived by Eqs. (6d)–(6f) and (14) as

$$(u^{(2)}_{pxq}, u^{(2)}_{pyq}, u^{(2)}_{pzq}) = (U^{(2)}_{pxq}, U^{(2)}_{pyq}, U^{(2)}_{pzq}) \exp\Big(\frac{2\mathrm{i}\omega}{c^{(2)}}(q_{p1}x_p + \beta_{pq}y_p + q_{p2}z_p)\Big), \tag{15}$$

where $U^{(2)}_{pxq}$, $U^{(2)}_{pyq}$, and $U^{(2)}_{pzq}$ are amplitudes for the double frequency, β_{pq} is the ratio of wave numbers for the second harmonic, and $c^{(2)} = \omega/k^{(2)}$ is the phase velocity of the second harmonic with $k^{(2)}$ denoting the wave number.

3 Band gap and transmission coefficient

We consider a 3D elastic wave in both the nonlinear phononic crystal and the elastic wave metamaterial. For the fundamental wave, we define the displacement and stress vectors as

$$\boldsymbol{u} = (u^{*(1)}_{pxq}, u^{*(1)}_{pyq}, u^{*(1)}_{pzq})^{\mathrm{T}}, \quad \boldsymbol{\sigma} = (\sigma^{*(1)}_{p12q}, \sigma^{*(1)}_{p22q}, \sigma^{*(1)}_{p23q})^{\mathrm{T}}, \tag{16}$$

where

$$u^{*(1)}_{pxq} = \sum_{q=1}^{6} U^{(1)}_{pxq} \exp\Big(\frac{\mathrm{i}\omega}{c^{(1)}}(q_{p1}x_p + \alpha_{pq}y_p + q_{p2}z_p)\Big), \tag{17a}$$

$$u^{*(1)}_{pyq} = \sum_{q=1}^{6} U^{(1)}_{pxq} a^{(1)}_{p2q} \exp\Big(\frac{\mathrm{i}\omega}{c^{(1)}}(q_{p1}x_p + \alpha_{pq}y_p + q_{p2}z_p)\Big), \tag{17b}$$

$$u^{*(1)}_{pzq} = \sum_{q=1}^{6} U^{(1)}_{pxq} a^{(1)}_{p3q} \exp\Big(\frac{\mathrm{i}\omega}{c^{(1)}}(q_{p1}x_p + \alpha_{pq}y_p + q_{p2}z_p)\Big), \tag{17c}$$

$$\sigma^{*(1)}_{p12q} = \sum_{q=1}^{6} \frac{\mathrm{i}\omega}{c^{(1)}} U^{(1)}_{pxq} G^{(1)}_{p1q} \exp\Big(\frac{\mathrm{i}\omega}{c^{(1)}}(q_{p1}x_p + \alpha_{pq}y_p + q_{p2}z_p)\Big), \tag{17d}$$

$$\sigma^{*(1)}_{p22q} = \sum_{q=1}^{6} \frac{\mathrm{i}\omega}{c^{(1)}} U^{(1)}_{pxq} G^{(1)}_{p2q} \exp\Big(\frac{\mathrm{i}\omega}{c^{(1)}}(q_{p1}x_p + \alpha_{pq}y_p + q_{p2}z_p)\Big), \tag{17e}$$

$$\sigma^{*(1)}_{p23q} = \sum_{q=1}^{6} \frac{\mathrm{i}\omega}{c^{(1)}} U^{(1)}_{pxq} G^{(1)}_{p3q} \exp\Big(\frac{\mathrm{i}\omega}{c^{(1)}}(q_{p1}x_p + \alpha_{pq}y_p + q_{p2}z_p)\Big). \tag{17f}$$

The state vectors at the left and right interfaces of each sub-cell for the nth unit cell can be written as

$$\boldsymbol{v}_{2n-1/2n^+} = \boldsymbol{T}_{p\mathrm{L}}(U^{(1)}_{px1}, U^{(1)}_{px2}, U^{(1)}_{px3}, U^{(1)}_{px4}, U^{(1)}_{px5}, U^{(1)}_{px6})^{\mathrm{T}} \exp\Big(\frac{\mathrm{i}\omega}{c^{(1)}}(q_{p1}x_p + q_{p2}z_p)\Big), \tag{18a}$$

$$\boldsymbol{v}_{2n^-/2n+1} = \boldsymbol{T}_{p\mathrm{R}}(U^{(1)}_{px1}, U^{(1)}_{px2}, U^{(1)}_{px3}, U^{(1)}_{px4}, U^{(1)}_{px5}, U^{(1)}_{px6})^{\mathrm{T}} \exp\Big(\frac{\mathrm{i}\omega}{c^{(1)}}(q_{p1}x_p + q_{p2}z_p)\Big), \tag{18b}$$

where $\boldsymbol{v}_{2n-1/2n^+/2n^-/2n+1} = (\boldsymbol{u}, \boldsymbol{\sigma})^{\mathrm{T}}_{2n-1/2n^+/2n^-/2n+1}$, and the detailed expressions of the coefficient matrices $\boldsymbol{T}_{p\mathrm{L}}$ and $\boldsymbol{T}_{p\mathrm{R}}$ are given in Appendix B.

According to the interfacial condition, we have the following relations:

$$\boldsymbol{v}_{2n^-} = \boldsymbol{T}_1 \boldsymbol{v}_{2n-1}, \quad \boldsymbol{v}_{2n+1} = \boldsymbol{T}_2 \boldsymbol{v}_{2n^+}, \tag{19}$$

where $\boldsymbol{T}_p$ ($p = 1, 2$) is the transfer matrix of each sub-cell with the following form:

$$\boldsymbol{T}_p = \boldsymbol{T}_{p\mathrm{R}} \boldsymbol{T}^{-1}_{p\mathrm{L}}. \tag{20}$$

Based on the constitutive equation, the stiffness matrices can be expressed as[42–43]

$$\begin{pmatrix}\boldsymbol{\sigma}_{2n-1}\\ \boldsymbol{\sigma}_{2n}\end{pmatrix}=\boldsymbol{K}_1\begin{pmatrix}\boldsymbol{u}_{2n-1}\\ \boldsymbol{u}_{2n}\end{pmatrix}, \tag{21a}$$

$$\begin{pmatrix}\boldsymbol{\sigma}_{2n}\\ \boldsymbol{\sigma}_{2n+1}\end{pmatrix}=\boldsymbol{K}_2\begin{pmatrix}\boldsymbol{u}_{2n}\\ \boldsymbol{u}_{2n+1}\end{pmatrix}, \tag{21b}$$

where $\boldsymbol{K}_p$ $(p=1,\,2)$ denotes the sub-cell stiffness matrix.

Then, the stiffness matrix can be derived from Eqs. (19)–(21) as

$$\boldsymbol{K}_p(6\times 6)=\begin{pmatrix}-\boldsymbol{T}_{pb}^{-1}\boldsymbol{T}_{pa} & \boldsymbol{T}_{pb}^{-1}\\ \boldsymbol{T}_{pb}-\boldsymbol{T}_{pd}\boldsymbol{T}_{pb}^{-1}\boldsymbol{T}_{pa} & \boldsymbol{T}_{pd}\boldsymbol{T}_{pb}^{-1}\end{pmatrix}, \tag{22}$$

where $\boldsymbol{T}_{p\zeta}$ $(\zeta=a,b,d)$ is the 3×3 sub-matrix of $\boldsymbol{T}_p$.

Eliminating the mechanical quantities at the $2n$th interface, the cell stiffness matrix can be derived as

$$\begin{pmatrix}\boldsymbol{\sigma}_{2n-1}\\ \boldsymbol{\sigma}_{2n+1}\end{pmatrix}=\boldsymbol{K}\begin{pmatrix}\boldsymbol{u}_{2n-1}\\ \boldsymbol{u}_{2n+1}\end{pmatrix}, \tag{23}$$

where

$$\boldsymbol{K}(6\times 6)=\begin{pmatrix}\boldsymbol{K}_{1a}+\boldsymbol{K}_{1b}(\boldsymbol{K}_{2a}-\boldsymbol{K}_{1d})^{-1}\boldsymbol{K}_{1c} & -\boldsymbol{K}_{1b}(\boldsymbol{K}_{2a}-\boldsymbol{K}_{1d})^{-1}\boldsymbol{K}_{2b}\\ \boldsymbol{K}_{2c}(\boldsymbol{K}_{2a}-\boldsymbol{K}_{1d})^{-1}\boldsymbol{K}_{1c} & \boldsymbol{K}_{2d}-\boldsymbol{K}_{2c}(\boldsymbol{K}_{2a}-\boldsymbol{K}_{1d})^{-1}\boldsymbol{K}_{2b}\end{pmatrix}, \tag{24}$$

and $\boldsymbol{K}_{p\zeta}$ $(\zeta=a,b,c,d)$ is the 3×3 sub-matrix of $\boldsymbol{K}_p$.

Then, the wave propagation in periodic structures satisfies the Bloch theorem as

$$\boldsymbol{v}_{2n+1}=\mathrm{e}^{\mathrm{i}kd}\boldsymbol{v}_{2n-1}, \tag{25}$$

where k refers to the wave number.

Based on Eqs. (23)–(25), the eigenvalue equation is expressed as

$$\left|\boldsymbol{T}-\mathrm{e}^{\mathrm{i}kd}\boldsymbol{I}\right|=0, \tag{26}$$

where

$$\boldsymbol{T}(6\times 6)=\begin{pmatrix}-\boldsymbol{K}_b^{-1}\boldsymbol{K}_a & \boldsymbol{K}_b^{-1}\\ \boldsymbol{K}_c-\boldsymbol{K}_d\boldsymbol{K}_b^{-1}\boldsymbol{K}_a & \boldsymbol{K}_d\boldsymbol{K}_b^{-1}\end{pmatrix}, \tag{27}$$

and $\boldsymbol{K}_\zeta$ $(\zeta=a,b,c,d)$ is the 3×3 sub-stiffness matrix of $\boldsymbol{K}$.

As a result, the band gap of the fundamental wave can be obtained by Eq. (26). As a result, the transmission coefficients of the fundamental wave can be calculated to support the band gap property. For the incident qS_2 wave, the displacements at the incident boundary consist of one incident wave and three reflected waves as

$$u_{x(1)}=U_{\mathrm{I}}r_{\mathrm{I}1}+U_{\mathrm{R}2}r_{\mathrm{I}2}+U_{\mathrm{R}4}r_{\mathrm{I}4}+U_{\mathrm{R}6}r_{\mathrm{I}6}, \tag{28a}$$

$$u_{y(1)}=U_{\mathrm{I}}a_{p21}^{(1)}r_{\mathrm{I}1}+U_{\mathrm{R}2}a_{p22}^{(1)}r_{\mathrm{I}2}+U_{\mathrm{R}4}a_{p24}^{(1)}r_{\mathrm{I}4}+U_{\mathrm{R}6}a_{p26}^{(1)}r_{\mathrm{I}6}, \tag{28b}$$

$$u_{z(1)}=U_{\mathrm{I}}a_{p31}^{(1)}r_{\mathrm{I}1}+U_{\mathrm{R}2}a_{p32}^{(1)}r_{\mathrm{I}2}+U_{\mathrm{R}4}a_{p34}^{(1)}r_{\mathrm{I}4}+U_{\mathrm{R}6}a_{p36}^{(1)}r_{\mathrm{I}6}, \tag{28c}$$

where the subscript (1) refers to the incident boundary, U_{I} is the amplitude of the incident

wave, $U_{\mathrm{R}2}$, $U_{\mathrm{R}4}$, and $U_{\mathrm{R}6}$ are the amplitudes of the reflected waves, and

$$r_{\mathrm{I}1} = \exp\Big(\frac{\mathrm{i}\omega}{c^{(1)}}(q_{p1}x_p + \alpha_{(1)1}y_p + q_{p2}z_p)\Big), \tag{29a}$$

$$r_{\mathrm{I}2} = \exp\Big(\frac{\mathrm{i}\omega}{c^{(1)}}(q_{p1}x_p + \alpha_{(1)2}y_p + q_{p2}z_p)\Big), \tag{29b}$$

$$r_{\mathrm{I}4} = \exp\Big(\frac{\mathrm{i}\omega}{c^{(1)}}(q_{p1}x_p + \alpha_{(1)4}y_p + q_{p2}z_p)\Big), \tag{29c}$$

$$r_{\mathrm{I}6} = \exp\Big(\frac{\mathrm{i}\omega}{c^{(1)}}(q_{p1}x_p + \alpha_{(1)6}y_p + q_{p2}z_p)\Big). \tag{29d}$$

The corresponding stresses can be expressed as

$$\sigma_{12(1)} = \frac{\mathrm{i}\omega}{c^{(1)}}(U_{\mathrm{I}}G^{(1)}_{p11}r_{\mathrm{I}1} + U_{\mathrm{R}2}G^{(1)}_{p12}r_{\mathrm{I}2} + U_{\mathrm{R}4}G^{(1)}_{p14}r_{\mathrm{I}4} + U_{\mathrm{R}6}G^{(1)}_{p16}r_{\mathrm{I}6}), \tag{30a}$$

$$\sigma_{22(1)} = \frac{\mathrm{i}\omega}{c^{(1)}}(U_{\mathrm{I}}G^{(1)}_{p21}r_{\mathrm{I}1} + U_{\mathrm{R}2}G^{(1)}_{p22}r_{\mathrm{I}2} + U_{\mathrm{R}4}G^{(1)}_{p24}r_{\mathrm{I}4} + U_{\mathrm{R}6}G^{(1)}_{p26}r_{\mathrm{I}6}), \tag{30b}$$

$$\sigma_{23(1)} = \frac{\mathrm{i}\omega}{c^{(1)}}(U_{\mathrm{I}}G^{(1)}_{p31}r_{\mathrm{I}1} + U_{\mathrm{R}2}G^{(1)}_{p32}r_{\mathrm{I}2} + U_{\mathrm{R}4}G^{(1)}_{p34}r_{\mathrm{I}4} + U_{\mathrm{R}6}G^{(1)}_{p36}r_{\mathrm{I}6}). \tag{30c}$$

At the transmitted boundary, the displacements are composed of three coupled waves along the forward direction as

$$u_{x(2)} = U_{\mathrm{T}1}r_{\mathrm{T}1} + U_{\mathrm{T}3}r_{\mathrm{T}3} + U_{\mathrm{T}5}r_{\mathrm{T}5}, \tag{31a}$$

$$u_{y(2)} = U_{\mathrm{T}1}a^{(1)}_{p21}r_{\mathrm{T}1} + U_{\mathrm{T}3}a^{(1)}_{p23}r_{\mathrm{T}3} + U_{\mathrm{T}5}a^{(1)}_{p25}r_{\mathrm{T}5}, \tag{31b}$$

$$u_{z(2)} = U_{\mathrm{T}1}a^{(1)}_{p31}r_{\mathrm{T}1} + U_{\mathrm{T}3}a^{(1)}_{p33}r_{\mathrm{T}3} + U_{\mathrm{T}5}a^{(1)}_{p35}r_{\mathrm{T}5}, \tag{31c}$$

where the subscript (2) denotes the transmitted boundary, $U_{\mathrm{T}1}$, $U_{\mathrm{T}3}$, and $U_{\mathrm{T}5}$ represent the amplitudes of transmitted waves, and

$$r_{\mathrm{T}1} = \exp\Big(\frac{\mathrm{i}\omega}{c^{(1)}}(q_{p1}x_p + \alpha_{(2)1}y_p + q_{p2}z_p)\Big), \tag{32a}$$

$$r_{\mathrm{T}3} = \exp\Big(\frac{\mathrm{i}\omega}{c^{(1)}}(q_{p1}x_p + \alpha_{(2)3}y_p + q_{p2}z_p)\Big), \tag{32b}$$

$$r_{\mathrm{T}5} = \exp\Big(\frac{\mathrm{i}\omega}{c^{(1)}}(q_{p1}x_p + \alpha_{(2)5}y_p + q_{p2}z_p)\Big). \tag{32c}$$

The stresses at the transmitted boundary can be given by

$$\sigma_{12(2)} = \frac{\mathrm{i}\omega}{c^{(1)}}(U_{\mathrm{T}1}G^{(1)}_{p11}r_{\mathrm{T}1} + U_{\mathrm{T}3}G^{(1)}_{p13}r_{\mathrm{T}3} + U_{\mathrm{T}5}G^{(1)}_{p15}r_{\mathrm{T}5}), \tag{33a}$$

$$\sigma_{22(2)} = \frac{\mathrm{i}\omega}{c^{(1)}}(U_{\mathrm{T}1}G^{(1)}_{p21}r_{\mathrm{T}1} + U_{\mathrm{T}3}G^{(1)}_{p23}r_{\mathrm{T}3} + U_{\mathrm{T}5}G^{(1)}_{p25}r_{\mathrm{T}5}), \tag{33b}$$

$$\sigma_{23(2)} = \frac{\mathrm{i}\omega}{c^{(1)}}(U_{\mathrm{T}1}G^{(1)}_{p31}r_{\mathrm{T}1} + U_{\mathrm{T}3}G^{(1)}_{p33}r_{\mathrm{T}3} + U_{\mathrm{T}5}G^{(1)}_{p35}r_{\mathrm{T}5}). \tag{33c}$$

The global stiffness matrix represents the relation of stress and displacement components at the incident and transmitted boundaries. The periodic structures contain m unit cells, and therefore we can derive the following relation[42–43]:

$$\begin{aligned}&\boldsymbol{K}^m(6\times 6)\\ &= \begin{pmatrix} \boldsymbol{K}_1^{m-1} + \boldsymbol{K}_2^{m-1}(\boldsymbol{K}_1^M - \boldsymbol{K}_4^{m-1})^{-1}\boldsymbol{K}_3^{m-1} & -\boldsymbol{K}_2^{m-1}(\boldsymbol{K}_1^M - \boldsymbol{K}_4^{m-1})^{-1}\boldsymbol{K}_2^M \\ \boldsymbol{K}_3^M(\boldsymbol{K}_1^M - \boldsymbol{K}_4^{m-1})^{-1}\boldsymbol{K}_3^{m-1} & \boldsymbol{K}_4^M - \boldsymbol{K}_3^M(\boldsymbol{K}_1^M - \boldsymbol{K}_4^{m-1})^{-1}\boldsymbol{K}_2^M \end{pmatrix},\end{aligned} \tag{34}$$

where $\boldsymbol{K}^m$ is the global stiffness matrix with m unit cells, $\boldsymbol{K}_\zeta^{m-1}$ denotes the sub-stiffness matrix with $m-1$ unit cells, and $\boldsymbol{K}_\zeta^M$ refers to the sub-stiffness matrix of the mth unit cell.

Then, combination of Eqs. (28)–(34) yields

$$\begin{pmatrix} \sigma_{12(1)} \\ \sigma_{22(1)} \\ \sigma_{23(1)} \\ \sigma_{12(2)} \\ \sigma_{22(2)} \\ \sigma_{23(2)} \end{pmatrix} = \boldsymbol{K}^m \begin{pmatrix} u_{x(1)} \\ u_{y(1)} \\ u_{z(1)} \\ u_{x(2)} \\ u_{y(2)} \\ u_{z(2)} \end{pmatrix}. \tag{35}$$

The reflection $\left(F_{\mathrm{RT2T2}} = \frac{U_{\mathrm{R2}}}{U_{\mathrm{I}}},\ F_{\mathrm{RT2T1}} = \frac{U_{\mathrm{R4}}}{U_{\mathrm{I}}},\ F_{\mathrm{RT2L}} = \frac{U_{\mathrm{R6}}}{U_{\mathrm{I}}}\right)$ and transmission $\left(F_{\mathrm{DT2T2}} = \frac{U_{\mathrm{T1}}}{U_{\mathrm{I}}},\ F_{\mathrm{DT2T1}} = \frac{U_{\mathrm{T3}}}{U_{\mathrm{I}}},\ F_{\mathrm{DT2L}} = \frac{U_{\mathrm{T5}}}{U_{\mathrm{I}}}\right)$ coefficients can be derived as

$$\eta = (\boldsymbol{K}^m \boldsymbol{M}_2 - \boldsymbol{M}_1)^{-1}(\boldsymbol{N}_1 - \boldsymbol{K}^m \boldsymbol{N}_2), \tag{36}$$

where $\eta = (F_{\mathrm{RT2T2}},\ F_{\mathrm{RT2T1}},\ F_{\mathrm{RT2L}},\ F_{\mathrm{DT2T2}},\ F_{\mathrm{DT2T1}},\ F_{\mathrm{DT2L}})$, and the elements of matrices $\boldsymbol{M}_1$, $\boldsymbol{M}_2$, $\boldsymbol{N}_1$, and $\boldsymbol{N}_2$ are presented in Appendix C. The results of the second harmonic can also be obtained by the previous derivation. The transmission coefficients of the second harmonic are denoted as H_{DT2T2}, H_{DT2T1}, and H_{DT2L} for the incident qS_2 wave and H_{DT1T2}, H_{DT1T1}, and H_{DT1L} for the incident qS_1 wave.

4 Numerical simulation and discussion

In this section, the numerical results of band gaps and transmission coefficients with initial stresses are presented. In Fig. 1(a), each unit cell is composed of nonlinear materials A and B whose material parameters were presented in Refs. [31] and [44]. The phononic crystal in the nonlinear elastic wave metamaterial consists of two different linear materials C and D[45]. These materials as the monoclinic media have 13 independent elastic constants[35].

Figures 2 and 3 show band gaps and transmission coefficients of the fundamental wave and the second harmonic in the nonlinear phononic crystal. The polar and azimuthal angles $\theta_1 = 26°$ and $\theta_2 = 25°$, the thickness ratio $d_1 : d_2 = 2 : 1$, and the phase velocities $c^{(1)} = c^{(2)} = 1\,510\,\mathrm{m/s}$ are considered. Figures 2(a)–2(c) show the effects of the normal initial stresses σ_{11}^0, σ_{22}^0, and σ_{33}^0 on the band gaps of the fundamental wave. We can see that the central frequency of band gaps increases with σ_{11}^0 and σ_{22}^0, but σ_{33}^0 gives the opposite influence. The transmission coefficients with $\sigma_{11}^0 = \sigma_{22}^0 = \sigma_{33}^0 = 1.5\,\mathrm{GPa}$ are calculated to support the band gap property in Figs. 2(d)–2(f). It is clear that the frequency regions with zero transmission coefficients correspond to the band gaps.

Figures 3(a)–3(c) illustrate the effects of the normal initial stresses in the 3D space on the band gaps of the second harmonic. It can be seen that the band gaps have a similar change by the initial stresses to the case of the fundamental wave. We can find that the initial stresses make the band gaps change evidently. Thus, the initial stress can be used as a tunable way for the band gaps of both the fundamental wave and the second harmonic. In Figs. 3(d)–3(i), the transmission coefficients with $\sigma_{11}^0 = \sigma_{22}^0 = \sigma_{33}^0 = 1.5\,\mathrm{GPa}$ for the incident qS_1 and qS_2 waves are presented, which agree well with the band gaps.

Figures 4 and 5 show the effects of the azimuthal angle θ_2 on the band gaps of the fundamental wave and the second harmonic for $\sigma_{11}^0 = 1.5\,\mathrm{GPa}$. In Fig. 4(a), the surface for the transmission coefficient F_{DT2T2} varying with the frequency and azimuthal angle is illustrated. As shown in Fig. 4(b), its contour clearly illustrates the relation of the azimuthal angle and the wave frequency. Figures 5(a) and 5(b) present the whole part and the contour of the transmission coefficient H_{DT2T1} for different azimuthal angles and wave frequencies. We can see that the locations of the band gaps shift towards the high frequency regions as the azimuthal angle increases for both the fundamental wave and the second harmonic. We can also see that the width of the second band gap changes slightly with the azimuthal angle. As a result, the central frequency of the band gap can be tuned by the initial stresses and the azimuthal angle.

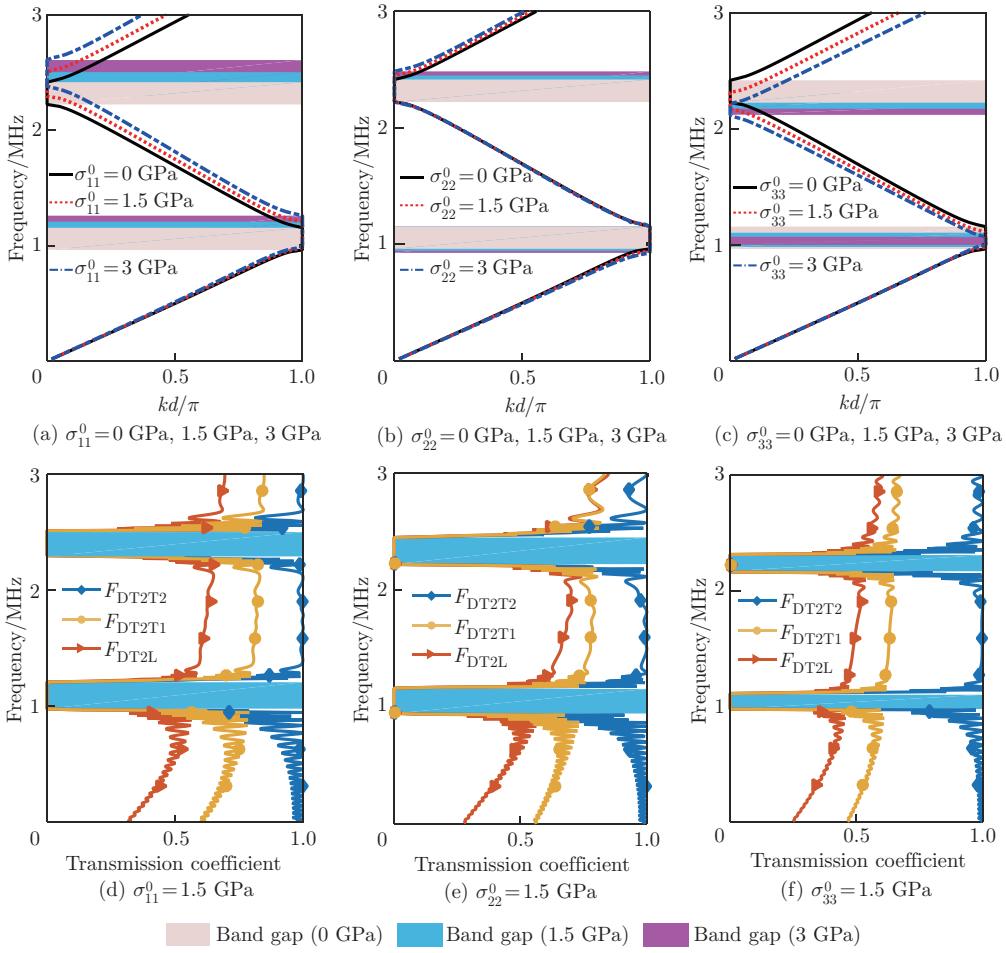

Fig. 2 Effects of the initial stresses on the band gaps of the fundamental wave, (a) $\sigma_{11}^0 = 0$ GPa, 1.5 GPa, 3 GPa, (b) $\sigma_{22}^0 = 0$ GPa, 1.5 GPa, 3 GPa, and (c) $\sigma_{33}^0 = 0$ GPa, 1.5 GPa, 3 GPa, and the transmission coefficients of the fundamental wave in the nonlinear phononic crystal with (d) $\sigma_{11}^0 = 1.5$ GPa, (e) $\sigma_{22}^0 = 1.5$ GPa, and (f) $\sigma_{33}^0 = 1.5$ GPa (color online)

Then, our attention is focused on achieving the 3D nonreciprocal transmission in the layered nonlinear elastic wave metamaterial. We consider the polar and azimuthal angles $\theta_1 = 26°$ and $\theta_2 = 20°$, the thickness ratio $d_1 : d_2 = 1 : 1$, and $c^{(1)} = c^{(2)} = 1\,350$ m/s. Figures 6(a) and 6(b) present the effects of the initial stress σ_{11}^0 on the band gaps of the fundamental wave and the second harmonic in the nonlinear elastic wave metamaterial. It can be seen that the central frequencies of band gaps for both elastic waves decrease with σ_{11}^0. It can also be seen from Fig. 6(b) that the influence of σ_{11}^0 on the band gaps in high frequency regions is more obvious.

Figures 7(a) and 7(b) show the band gaps of the fundamental wave and the second harmonic with $\sigma_{11}^0 = 3$ GPa. It can be seen that the frequency regions of band gaps are 0.38 MHz–0.58 MHz for the fundamental wave, as well as 0.19 MHz–0.29 MHz and 0.46 MHz–0.52 MHz for the second harmonic. As a result, the frequency region of the nonreciprocal transmission is 0.38 MHz–0.46 MHz, i.e., the fundamental wave is located at the stop band, while the second harmonic falls in the pass band.

Figure 8 illustrates the nonreciprocal transmission of the 3D waves for the incident qS_2 wave in the positive direction. Figure 8(a) shows the transmission coefficients of the fundamental wave, while Figs. 8(b) and 8(c) illustrate the transmission coefficients of the second harmonic.

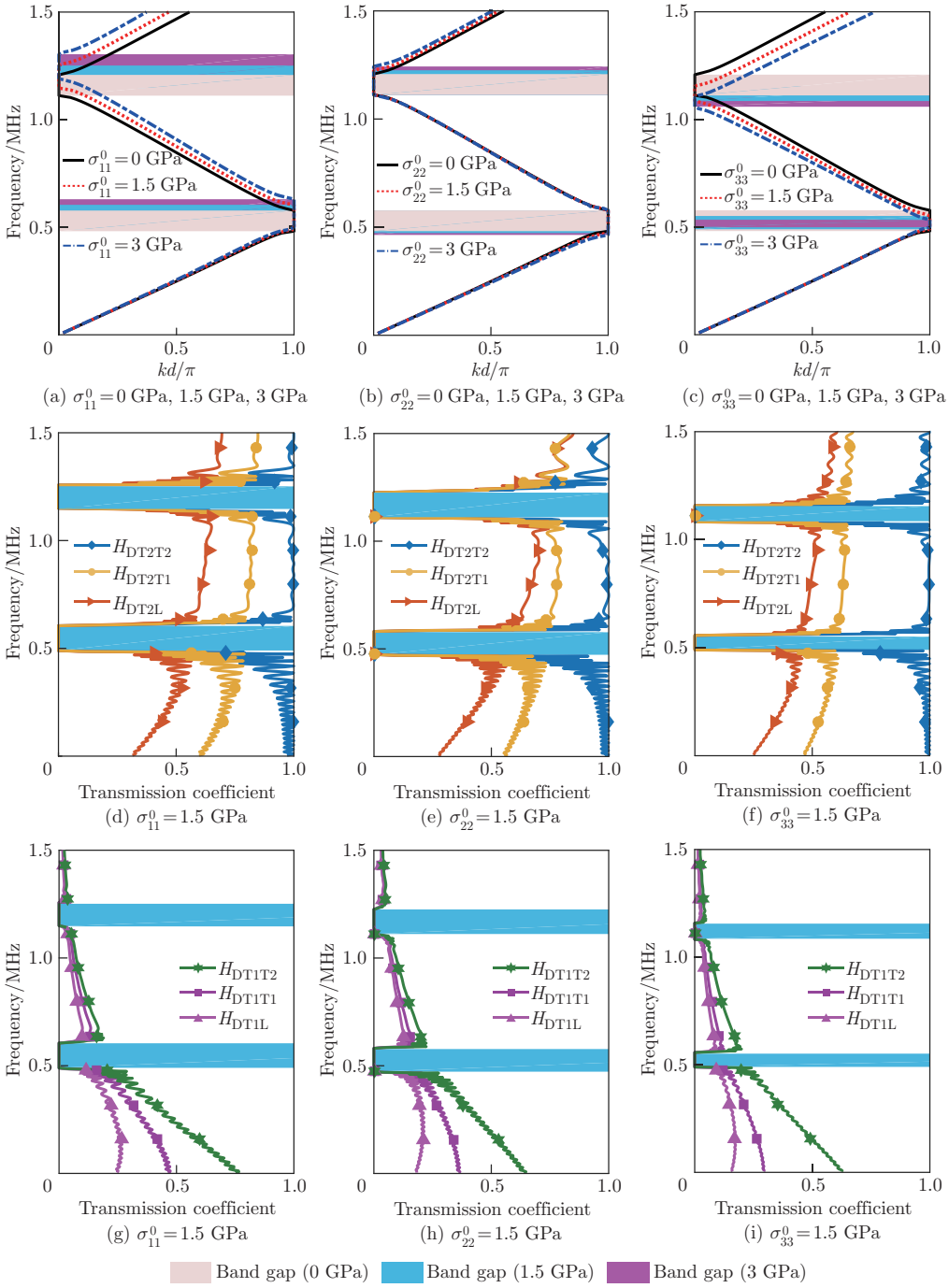

(a) σ_{11}^0=0 GPa, 1.5 GPa, 3 GPa (b) σ_{22}^0=0 GPa, 1.5 GPa, 3 GPa (c) σ_{33}^0=0 GPa, 1.5 GPa, 3 GPa

(d) σ_{11}^0=1.5 GPa (e) σ_{22}^0=1.5 GPa (f) σ_{33}^0=1.5 GPa

(g) σ_{11}^0=1.5 GPa (h) σ_{22}^0=1.5 GPa (i) σ_{33}^0=1.5 GPa

Fig. 3 Effects of the initial stresses on the band gaps of the second harmonic, (a) $\sigma_{11}^0 = 0$ GPa, 1.5 GPa, 3 GPa, (b) $\sigma_{22}^0 = 0$ GPa, 1.5 GPa, 3 GPa, and (c) $\sigma_{33}^0 = 0$ GPa, 1.5 GPa, 3 GPa, the transmission coefficients of the second harmonic for the incident qS_2 wave with (d) $\sigma_{11}^0 = 1.5$ GPa, (e) $\sigma_{22}^0 = 1.5$ GPa, and (f) $\sigma_{33}^0 = 1.5$ GPa, and the transmission coefficients of the second harmonic in the nonlinear phononic crystal for the incident qS_1 wave with (g) $\sigma_{11}^0 = 1.5$ GPa, (h) $\sigma_{22}^0 = 1.5$ GPa, and (i) $\sigma_{33}^0 = 1.5$ GPa (color online)

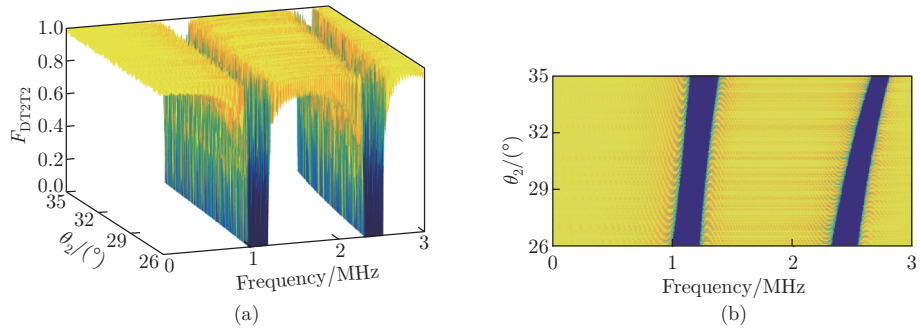

Fig. 4 Transmission coefficient of the fundamental wave F_{DT2T2} in the nonlinear phononic crystal with $\sigma_{11}^0 = 1.5\,\text{GPa}$ for different azimuthal angles θ_2: (a) the transmission coefficient F_{DT2T2} varying with both the azimuthal angle and the frequency and (b) its contour in the azimuthal angle versus the frequency plane (color online)

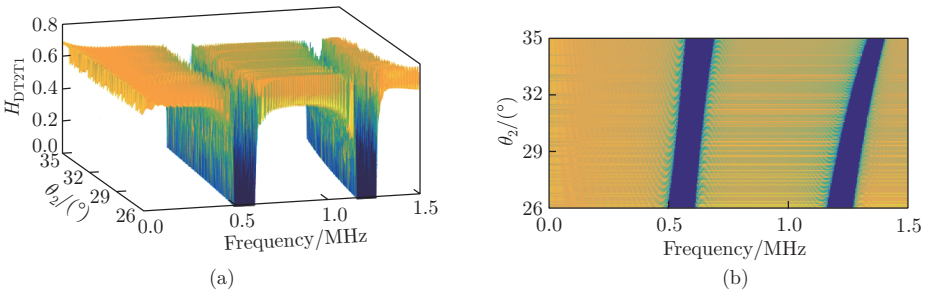

Fig. 5 Transmission coefficient of the second harmonic H_{DT2T1} in the nonlinear phononic crystal with $\sigma_{11}^0 = 1.5\,\text{GPa}$ for different azimuthal angles θ_2: (a) the transmission coefficient H_{DT2T1} varying with both the azimuthal angle and the frequency and (b) its contour in the azimuthal angle versus the frequency plane (color online)

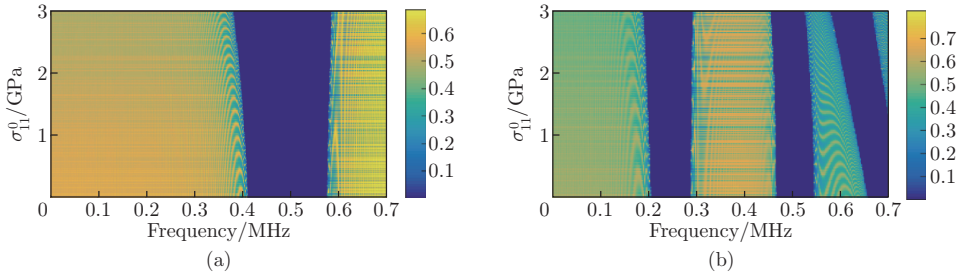

Fig. 6 Transmission coefficients of (a) the fundamental wave (F_{DT2T2}) and (b) the second harmonic (H_{DT2T2}) changing with both σ_{11}^0 and the frequency in the nonlinear elastic wave metamaterial (color online)

We can see that the transmission coefficients of the fundamental wave remain zero but the results of the second harmonic are not zero in the region 0.38 MHz–0.46 MHz. The frequency region of the nonreciprocal transmission without initial stresses is 0.41 MHz–0.47 MHz. We find that the initial stress σ_{11}^0 makes the central frequency of the nonreciprocal transmission change and the gap width increase about 0.2 MHz.

For the incident qS_2 wave in the negative direction, the transmission coefficient of the second harmonic is zero in the nonreciprocal frequency region. It is mainly because the second harmonic cannot be generated in the linear materials and the fundamental wave is located at the stop band. Thus, the transmission coefficients with initial stresses for both the fundamental wave

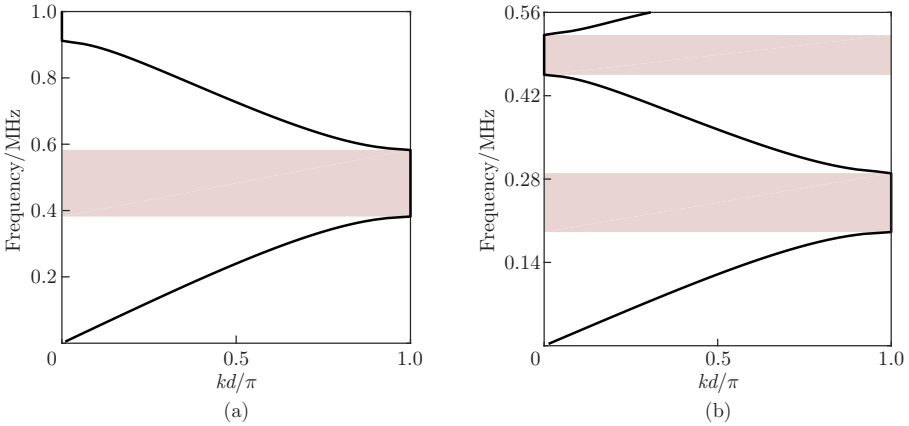

Fig. 7 Band gaps of the fundamental wave and the second harmonic in the nonlinear elastic wave metamaterial with $\sigma_{11}^0 = 3\,\mathrm{GPa}$: (a) fundamental wave and (b) second harmonic (color online)

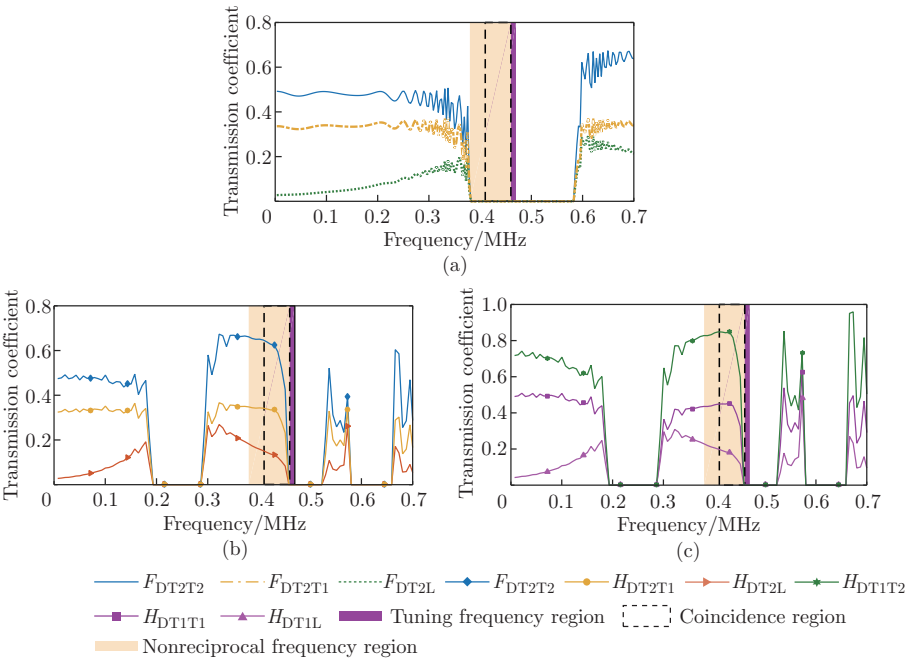

Fig. 8 Nonreciprocal transmission of the incident elastic wave along the positive direction with $\sigma_{11}^0 = 3\,\mathrm{GPa}$: (a) the fundamental wave and the transmission coefficients of the second harmonic for the incident (b) qS_2 and (c) qS_1 wave modes (color online)

and the second harmonic are zero in the frequency region 0.38 MHz–0.46 MHz. As a result, the nonreciprocal phenomenon in the 3D space can be achieved, which permits the wave propagation only along the positive direction. Then, we can tune the location and width of the frequency region for the 3D nonreciprocal transmission by initial stresses.

5 Conclusions

In this work, the effects of the initial stresses on the wave propagation of 3D waves in both nonlinear phononic crystal and elastic wave metamaterial are studied. The analytical solutions for the coupled qP, qS_1, and qS_2 waves with the initial stresses are derived. The band gaps

and transmission coefficients of the fundamental wave and second harmonic are obtained by the transfer and stiffness matrices. The nonreciprocal transmission for an incident 3D wave can be achieved in the nonlinear elastic wave metamaterial with initial stresses. We can find that the initial stresses can tune the frequency regions of the band gap and nonreciprocal transmission in layered periodic structures. This work is expected to be helpful for designing devices of the nonreciprocal transmission with vector and tunable properties.

References

[1] KHELIF, A., AOUBIZA, B., MOHAMMADI, S., ADIBI, A., and LAUDE, V. Complete band gaps in two-dimensional phononic crystal slabs. *Physical Review E*, **74**, 046610 (2006)

[2] KUTSENKO, A. A., SHUVALOV, A. L., and NORRIS, A. N. Evaluation of the effective speed of sound in phononic crystals by the monodromy matrix method. *Journal of the Acoustical Society of America*, **130**, 3553–3557 (2011)

[3] KUTSENKO, A. A., SHUVALOV, A. L., and NORRIS, A. N. Converging bounds for the effective shear speed in 2D phononic crystals. *Journal of Elasticity*, **113**, 179–191 (2013)

[4] JANDRON, M. and HENANN, D. L. A numerical simulation capability for electroelastic wave propagation in dielectric elastomer composites: application to tunable soft phononic crystals. *International Journal of Solids and Structures*, **150**, 1–21 (2018)

[5] MADEO, A., COLLET, M., MINIACI, M., BILLON, K., OUISSE, M., and NEFF, P. Modeling phononic crystals via the weighted relaxed micromorphic model with free and gradient micro-inertia. *Journal of Elasticity*, **130**, 59–83 (2018)

[6] LAZAROV, B. S. and JENSEN, J. S. Low-frequency band gaps in chains with attached non-linear oscillators. *International Journal of Non-Linear Mechanics*, **42**, 1186–1193 (2007)

[7] VONDREJC, J., ROHAN, E., and HECZKO, J. Shape optimization of phononic band gap structures using the homogenization approach. *International Journal of Solids and Structures*, **113**, 147–168 (2017)

[8] DOMINO, L., TARPIN, M., PATINET, S., and EDDI, A. Faraday wave lattice as an elastic metamaterial. *Physical Review E*, **93**, 050202 (2016)

[9] WEI, C. Q., YAN, Z. Z., ZHENG, H., and ZHANG, C. Z. RBF collocation method and stability analysis for phononic crystals. *Applied Mathematics and Mechanics* (*English Edition*), **37**(5), 627–638 (2016) https://doi.org/10.1007/s10483-016-2076-8

[10] MO, C. Y., SINGH, J., RANEY, J. R., and PUROHIT, P. K. Cnoidal wave propagation in an elastic metamaterial. *Physical Review E*, **100**, 013001 (2019)

[11] MIRANDA, E. J. P. and DOS SANTOS, J. M. C. Flexural wave band gaps in multi-resonator elastic metamaterial Timoshenko beams. *Wave Motion*, **91**, 102391 (2019)

[12] WU, Z. J., LIU, W. Y., LI, F. M., and ZHANG, C. Band-gap property of a novel elastic metamaterial beam with X-shaped local resonators. *Mechanical Systems and Signal Processing*, **134**, 106357 (2019)

[13] BEHRAVAN-RAD, A. and JAFARI, M. Hygroelasticity analysis of an elastically restrained functionally graded porous metamaterial circular plate resting on an auxetic material circular plate. *Applied Mathematics and Mechanics* (*English Edition*), **41**(9), 1359–1380 (2020) https://doi.org/10.1007/s10483-020-2651-7

[14] ZHAO, P. C., ZHANG, K., ZHAO, C., and DENG, Z. C. Multi-resonator coupled metamaterials for broadband vibration suppression. *Applied Mathematics and Mechanics* (*English Edition*), **42**(1), 53–64 (2021) https://doi.org/10.1007/s10483-021-2684-8

[15] EL-BORGI, S., FERNANDES, R., RAJENDRAN, P., YAZBECK, R., BOYD, J. G., and LAGOUDAS, D. C. Multiple bandgap formation in a locally resonant linear metamaterial beam: theory and experiments. *Journal of Sound and Vibration*, **488**, 115647 (2020)

[16] DENG, M. X. and XIANG, Y. X. Analysis of second-harmonic generation by primary horizontal shear modes in layered planar structures with imperfect interfaces. *Journal of Applied Physics*, **113**, 043513 (2013)

[17] IWAI, A., NAKAMURA, Y., and SAKAI, O. Enhanced generation of a second-harmonic wave in a composite of metamaterial and microwave plasma with various permittivities. *Physical Review E*, **92**, 033105 (2015)

[18] LI, Y. F., LAN, J., LI, B. S., LIU, X. Z., and ZHANG, J. S. Nonlinear effects in an acoustic metamaterial with simultaneous negative modulus and density. *Journal of Applied Physics*, **120**, 145105 (2016)

[19] CHAUNSALI, R., TOLES, M., YANG, J. Y., and KIM, E. Extreme control of impulse transmission by cylinder-based nonlinear phononic crystals. *Journal of the Mechanics and Physics of Solids*, **107**, 21–32 (2017)

[20] BANERJEE, A., CALIUS, E. P., and DAS, R. Impact based wideband nonlinear resonating metamaterial chain. *International Journal of Non-Linear Mechanics*, **103**, 138–144 (2018)

[21] LIANG, B., ZOU, X. Y., YUAN, B., and CHENG, J. C. Frequency-dependence of the acoustic rectifying efficiency of an acoustic diode model. *Applied Physics Letters*, **96**, 233511 (2010)

[22] LIANG, B., GUO, X. S., TU, J., ZHANG, D., and CHENG, J. C. An acoustic rectifier. *Nature Materials*, **9**, 989–992 (2010)

[23] BOECHLER, N., THEOCHARIS, G., and DARAIO, C. Bifurcation-based acoustic switching and rectification. *Nature Materials*, **10**, 665–668 (2011)

[24] LI, X. F., NI, X., FENG, L., LU, M. H., HE, C., and CHEN, Y. F. Tunable unidirectional sound propagation through a sonic-crystal-based acoustic diode. *Physical Review Letters*, **106**, 084301 (2011)

[25] LUO, B. B., GAO, S., LIU, J. H., MAO, Y. W., LI, Y. F., and LIU, X. Z. Nonreciprocal wave propagation in one-dimensional nonlinear periodic structures. *AIP Advances*, **8**, 015113 (2018)

[26] GRINBERG, I., VAKAKIS, A. F., and GENDELMAN, O. V. Acoustic diode: wave non-reciprocity in nonlinearly coupled waveguides. *Wave Motion*, **83**, 49–66 (2018)

[27] KONARSKI, S. G., HABERMAN, M. R., and HAMILTON, M. F. Frequency-dependent behavior of media containing pre-strained nonlinear inclusions: application to nonlinear acoustic metamaterials. *Journal of the Acoustical Society of America*, **144**, 3022–3035 (2018)

[28] DARABI, A., FANG, L. Z., MOJAHED, A., FRONK, M. D., VAKAKIS, A. F., and LEAMY, M. J. Broadband passive nonlinear acoustic diode. *Physical Review B*, **99**, 214305 (2019)

[29] CHEN, Y. J., WU, B., SU, Y. P., and CHEN, W. Q. Tunable two-way unidirectional acoustic diodes: design and simulation. *Journal of Applied Mechanics*, **86**, 031010 (2019)

[30] WALLEN, S. P. and HABERMAN, M. R. Nonreciprocal wave phenomena in spring-mass chains with effective stiffness modulation induced by geometric nonlinearity. *Physical Review E*, **99**, 031001 (2019)

[31] CHATTERJEE, M., DHUA, S., CHATTOPADHYAY, A., and SAHU, S. A. Reflection and refraction for three-dimensional plane waves at the interface between distinct anisotropic half-spaces under initial stresses. *International Journal of Geomechanics*, **16**, 04015099 (2016)

[32] ZHANG, Z., HAN, X. K., and JI, G. M. Mechanism for controlling the band gap and the flat band in three component phononic crystals. *Journal of Physics and Chemistry of Solids*, **123**, 235–241 (2018)

[33] GUO, X., JI, S. S., LIU, H., and REN, K. Dispersion relations of elastic waves in three-dimensional cubical piezoelectric phononic crystal with initial stresses and mechanically and dielectrically imperfect interfaces. *Applied Mathematical Modelling*, **69**, 405–424 (2019)

[34] FOMENKO, S. I., GOLUB, M. V., CHEN, A., WANG, Y. S., and ZHANG, C. Band-gap and pass-band classification for oblique waves propagating in a three-dimensional layered functionally graded piezoelectric phononic crystal. *Journal of Sound and Vibration*, **439**, 219–240 (2019)

[35] LI, Z. N., WANG, Y. Z., and WANG, Y. S. Three-dimensional nonreciprocal transmission in a layered nonlinear elastic wave metamaterial. *International Journal of Non-Linear Mechanics*, **125**, 103531 (2020)

[36] WANG, Y. Z., LI, F. M., and KISHIMOTO, K. Effects of the initial stress on the propagation and localization properties of Rayleigh waves in randomly disordered layered piezoelectric phononic crystals. *Acta Mechanica*, **216**, 291–300 (2011)

[37] GUO, X. and WEI, P. J. Dispersion relations of elastic waves in one-dimensional piezoelectric phononic crystal with initial stresses. *International Journal of Mechanical Sciences*, **106**, 231–244 (2016)

[38] BARNWELL, E. G., PARNELL, W. J., and ABRAHAMS, I. D. Antiplane elastic wave propagation in pre-stressed periodic structures; tuning, band gap switching and invariance. *Wave Motion*, **63**, 98–110 (2016)

[39] ROSE, J. L. *Ultrasonic Waves in Solid Media*, Cambridge University Press, Cambridge (1999)

[40] NORRIS, A. N. Symmetry conditions for third order elastic moduli and implications in nonlinear wave theory. *Journal of Elasticity*, **25**, 247–257 (1991)

[41] DENG, M. X. Cumulative second-harmonic generation of Lamb-mode propagation in a solid plate. *Journal of Applied Physics*, **85**, 3051–3058 (1999)

[42] ROKHLIN, S. I. and WANG, L. Stable recursive algorithm for elastic wave propagation in layered anisotropic media: stiffness matrix method. *Journal of the Acoustical Society of America*, **112**, 822–834 (2002)

[43] TAN, E. L. Stiffness matrix method with improved efficiency for elastic wave propagation in layered anisotropic media. *Journal of the Acoustical Society of America*, **118**, 3400–3403 (2005)

[44] CHATTOPADHYAY, A. Wave reflection and refraction in triclinic crystalline media. *Archive of Applied Mechanics*, **73**, 568–579 (2004)

[45] QUINTANILLA, F. H., LOWE, M. J. S., and CRASTER, R. V. Full 3D dispersion curve solutions for guided waves in generally anisotropic media. *Journal of Sound and Vibration*, **363**, 545–559 (2016)

Appendix A

The expressions of A_6, A_4, A_2, and A_0 in Eq. (10) are

$$A_6 = C_{p22}C_{p44}S_{21} - C_{p22}C_{p66}S_{32} + C_{p22}C_{p44}C_{p66} - C_{p22}C_{p46}^2 - C_{p22}S_{21}S_{32}, \tag{A1}$$

$$\begin{aligned}A_4 = {}& \rho_p S_{21}S_{32}(c^{(1)})^2 - C_{p22}\rho_p S_{21}(c^{(1)})^2 - S_{21}C_{p44}\rho_p(c^{(1)})^2 + S_{21}C_{p22}C_{p33}q_{p2}^2 - S_{21}S_{31}C_{p22}q_{p1}^2 \\ & + 2S_{21}C_{p22}C_{p35}q_{p1}q_{p2} + S_{21}C_{p22}C_{p55}q_{p1}^2 - S_{21}C_{p23}^2q_{p2}^2 - 2S_{21}C_{p23}C_{p25}q_{p1}q_{p2} - S_{21}C_{p25}^2q_{p1}^2 \\ & - 2S_{21}C_{p23}C_{p44}q_{p2}^2 - 2S_{21}C_{p23}C_{p46}q_{p1}q_{p2} - 2S_{21}C_{p25}C_{p44}q_{p1}q_{p2} - 2S_{21}C_{p25}C_{p46}q_{p1}^2 \\ & - 2S_{21}C_{p25}C_{p46}q_{p1}^2 - S_{31}S_{32}C_{p22}q_{p2}^2 + S_{31}C_{p22}C_{p44}q_{p2}^2 - S_{31}C_{p22}C_{p66}q_{p1}^2 + S_{32}C_{p22}\rho_p(c^{(1)})^2 \\ & + S_{32}C_{p66}\rho_p(c^{(1)})^2 - S_{32}C_{p11}C_{p22}q_{p1}^2 + S_{32}C_{p12}^2q_{p1}^2 + 2S_{32}C_{p12}C_{p25}q_{p1}q_{p2} + S_{32}C_{p25}^2q_{p2}^2 \\ & + 2S_{32}C_{p12}C_{p66}q_{p1}^2 - 2S_{32}C_{p15}C_{p22}q_{p1}q_{p2} - S_{32}C_{p22}C_{p55}q_{p2}^2 + 2S_{32}C_{p25}C_{p46}q_{p2}^2 \\ & + 2S_{32}C_{p25}C_{p66}q_{p1}q_{p2} - C_{p66}\rho_p(c^{(1)})^2(C_{p44}+C_{p22}) + C_{p46}^2\rho_p(c^{(1)})^2 - C_{p12}^2C_{p44}q_{p1}^2 \\ & + C_{p11}C_{p22}C_{p44}q_{p1}^2 + 2C_{p12}q_{p1}q_{p2}(C_{p23}C_{p46} - C_{p25}C_{p44}) - 2C_{p13}C_{p22}C_{p46}q_{p1}q_{p2} \\ & + 2C_{p12}q_{p1}^2(C_{p25}C_{p46} - C_{p44}C_{p66}) + 2C_{p15}C_{p22}C_{p44}q_{p1}q_{p2} - 2C_{p15}C_{p22}C_{p46}q_{p1}^2 \\ & + 2C_{p12}C_{p46}^2q_{p1}^2 + C_{p22}C_{p33}C_{p66}q_{p2}^2 + 2C_{p22}C_{p35}(C_{p66}q_{p1}q_{p2} - C_{p46}q_{p2}^2) - C_{p66}C_{p23}^2q_{p2}^2 \\ & + C_{p22}C_{p55}(C_{p44}q_{p2}^2 - 2C_{p46}q_{p1}q_{p2} + C_{p66}q_{p1}^2) + 2C_{p23}q_{p2}^2(C_{p25}C_{p46} - C_{p44}C_{p66}) \\ & + 2C_{p23}C_{p46}^2q_{p2}^2 - 2C_{p23}C_{p25}C_{p66}q_{p1}q_{p2} - C_{p25}^2(C_{p44}q_{p2}^2 + 2C_{p46}q_{p1}q_{p2} - C_{p66}q_{p1}^2) \\ & - 4C_{p25}C_{p44}C_{p66}q_{p1}q_{p2} + 4C_{p25}C_{p46}^2q_{p1}q_{p2} + 2S_{32}C_{p12}C_{p46}q_{p1}q_{p2},\end{aligned} \tag{A2}$$

$$\begin{aligned}A_2 = {}& S_{21}S_{31}(\rho_p q_{p1}^2(c^{(1)})^2 - 2(C_{p23}-2C_{p44})q_{p1}^2q_{p2}^2 - 2(C_{p25}+2C_{p46})q_{p1}^3q_{p2}) + S_{21}S_{32}(C_{p11}q_{p1}^4 \\ & - \rho_p(c^{(1)})^2(q_{p1}^2+q_{p2}^2) + 2q_{p1}^2q_{p2}^2(C_{p13}+2C_{p55}) + 4C_{p15}q_{p1}^3q_{p2} + C_{p33}q_{p2}^4 + 4C_{p35}q_{p2}^3q_{p1})\end{aligned}$$

$$
\begin{aligned}
&+ S_{21}((\rho_p)^2(c^{(1)})^2(1 - q_{p2}^2(C_{p33} + C_{p44}) - 2q_{p1}q_{p2}(C_{p35} + C_{p46}) + C_{p44}q_{p1}^2 - C_{p55}q_{p1}^2)\\
&- (C_{p11}C_{p44} - 2C_{p15}C_{p46})q_{p1}^4 + 2q_{p1}^3q_{p2}(C_{p13}C_{p46} - C_{p15}C_{p44} + 2C_{p46}C_{p55}) + C_{p33}C_{p44}q_{p2}^4\\
&+ 2q_{p1}q_{p2}^3(C_{p33}C_{p46} + C_{p35}C_{p44}) + 6C_{p35}C_{p46}q_{p1}^2q_{p2}^2) + S_{31}S_{32}(\rho_p c^{(1)}q_{p2}^2 - 2C_{p12}q_{p1}^2q_{p2}^2\\
&- 2q_{p1}q_{p2}^3(C_{p25} + 2C_{p46}) - 4C_{p66}q_{p1}^2q_{p2}^2) + S_{31}(\rho_p(c^{(1)})^2(C_{p22}(q_{p1}^2 - q_{p2}^2) - C_{p44}q_{p2}^2\\
&+ C_{p66}q_{p1}^2) + (C_{p11}C_{p22} + 2C_{p12}C_{p66} + C_{p12}^2)q_{p1}^4 + 2q_{p1}^3q_{p2}(C_{p12}(C_{p25} + C_{p46}) + C_{p15}C_{p22})\\
&+ q_{p2}^4(C_{p22}C_{p33} - C_{p23}^2 - 2C_{p23}C_{p44}) + 2q_{p1}q_{p2}^3(C_{p22}C_{p35} - C_{p23}(C_{p25} + C_{p46}) - C_{p25}C_{p44})\\
&+ 2C_{p25}C_{p66}q_{p1}^3q_{p2}) + S_{32}((c^{(1)})^2\rho_p((C_{p11} + C_{p66})q_{p1}^2 + 2q_{p1}q_{p2}(C_{p15} + C_{p46}) + C_{p55}q_{p2}^2\\
&- C_{p66}q_{p2}^2) - 2q_{p1}^3q_{p2}(C_{p11}C_{p46} + C_{p15}C_{p66}) + 2q_{p1}q_{p2}^3(C_{p35}C_{p66} - C_{p46}(C_{p13} + 2C_{p55}))\\
&+ (C_{p33}C_{p66} - 2C_{p35}C_{p46})q_{p2}^4 - 6C_{p15}C_{p46}q_{p1}^2q_{p2}^2 - C_{p11}C_{p66}q_{p1}^4) + (c^{(1)})^4\rho_p^2(C_{p22} - S_{31}\\
&+ C_{p44} + C_{p66}) + (c^{(1)})^2\rho_p((C_{p12}^2 - C_{p11}(C_{p22} + C_{p44}) + 2C_{p46}(C_{p15} + C_{p25}) + 2C_{p12}C_{p66}\\
&+ C_{p25}^2 - C_{p22}C_{p55} - (C_{p55} + C_{p44})C_{p66} + C_{p46}^2)q_{p1}^2 + 2q_{p1}q_{p2}(C_{p12}(C_{p25} + C_{p46}) + C_{p46}(C_{p13}\\
&+ C_{p55}) + C_{p15}(C_{p22} - C_{p44}) - C_{p35}(C_{p22} + C_{p66}) + C_{p23}(C_{p25} + C_{p46}) + C_{p25}(C_{p44} + C_{p66}))\\
&+ q_{p2}^2(C_{p23}^2 + 2C_{p23}C_{p44} - C_{p22}(C_{p33} + C_{p55}) + 2C_{p46}(C_{p25} + C_{p35}) - C_{p44}(C_{p55} + C_{p66})\\
&- C_{p33}C_{p66} + C_{p25}^2 + C_{p46}^2)) + q_{p1}^2q_{p2}^2(C_{p11}(C_{p22}C_{p33} - C_{p23}^2 - 2C_{p23}C_{p44}) - C_{p33}C_{p12}^2\\
&+ 2C_{p12}(C_{p13}(C_{p44} + C_{p23}) + C_{p55}(C_{p23} + C_{p44}) - C_{p35}(C_{p25} + C_{p46}) - C_{p33}C_{p66}) - C_{p22}C_{p13}^2\\
&+ 2C_{p15}(C_{p22}C_{p35} - C_{p23}(C_{p25} + C_{p46}) - C_{p25}C_{p44}) + 2C_{p66}((C_{p23} + C_{p44})C_{p55} - C_{p25}C_{p35})\\
&+ 2C_{p13}(C_{p66}(C_{p44} + C_{p23}) - C_{p22}C_{p55} - C_{p46}^2 + C_{p25}^2 + 2C_{p25}C_{p46}) - 4C_{p55}C_{p46}^2)\\
&+ q_{p1}^4(2C_{p12}(C_{p15}(C_{p25} + C_{p46}) - C_{p55}(C_{p66} + C_{p12})) + 2C_{p25}(C_{p15}C_{p66} - C_{p11}C_{p46})\\
&- 2C_{p22}(C_{p15}^2 - C_{p11}C_{p55}) + C_{p11}(C_{p44}C_{p66} - C_{p25}^2 - C_{p46}^2)) + 2q_{p1}^3q_{p2}(C_{p12}C_{p15}(C_{p23} + C_{p44})\\
&+ (C_{p12}C_{p13} - C_{p11}C_{p23})(C_{p25} + C_{p46}) + 2C_{p15}(C_{p44}C_{p66} - C_{p46}^2) + C_{p66}(C_{p13}C_{p25} + C_{p15}C_{p23})\\
&+ C_{p11}(C_{p22}C_{p35} - C_{p25}C_{p44}) - C_{p12}C_{p35}(C_{p12} + 2C_{p66}) - C_{p13}C_{p15}C_{p22}) - 2q_{p1}q_{p2}^3(2C_{p35}C_{p46}^2\\
&- C_{p12}C_{p35}(C_{p23} + C_{p44}) + (C_{p12}C_{p33} - C_{p13}C_{p23})(C_{p25} + C_{p46}) + C_{p15}C_{p23}(C_{p23} + 2C_{p44})\\
&+ C_{p13}(C_{p22}C_{p35} - C_{p25}C_{p44}) - C_{p35}C_{p66}(C_{p23} + C_{p44}) + C_{p33}(C_{p25}C_{p66} - C_{p15}C_{p22}))\\
&+ q_{p2}^4(2C_{p35}(C_{p23}(C_{p25} + C_{p46}) + C_{p25}C_{p44}) - C_{p23}C_{p55}(C_{p23} + 2C_{p44}) - C_{p22}C_{p35}^2\\
&+ C_{p33}(C_{p22}C_{p55} + C_{p44}C_{p66} - C_{p25}(C_{p25} + 2C_{p46}) - C_{p46}^2)),
\end{aligned}
\tag{A3}
$$

$$
\begin{aligned}
A_0 = {}& S_{21}((c^{(1)})^2\rho_p(q_{p1}^2q_{p2}^2(S_{31} + C_{p33} + C_{p55}) + q_{p1}^4(C_{p11} - S_{31} + C_{p55}) + 2q_{p1}^3q_{p2}(C_{p15} + C_{p35}))\\
&+ q_{p1}^6((S_{31} - C_{p55})C_{p11} + C_{p15}^2) - 2q_{p1}^3q_{p2}^3((S_{31} + C_{p13})C_{p35} + C_{p15}C_{p33}) + q_{p1}^4q_{p2}^2(C_{p13}^2\\
&+ 2C_{p13}C_{p55} - C_{p11}C_{p33} - 2C_{p15}C_{p35}) + 2q_{p1}^5q_{p2}((C_{p13} + S_{31})C_{p15} - C_{p11}C_{p35}) + q_{p1}^2q_{p2}^4(C_{p35}^2\\
&- (S_{31} + C_{p55})C_{p33}) - (c^{(1)})^4\rho_p^2q_{p1}^2) + S_{31}((c^{(1)})^2\rho_p(q_{p1}^2q_{p2}^2(S_{32} + C_{p44} - C_{p66}) + 2q_{p1}^3q_{p2}(C_{p15}\\
&+ C_{p46}) - 2q_{p1}q_{p2}^3(C_{p35} + C_{p46}) - q_{p2}^4(S_{32} + C_{p33} + C_{p44}) + q_{p1}^4(C_{p11} + C_{p66}) + q_{p6}^4(S_{32}C_{p33}\\
&+ C_{p33}C_{p44})) - (c^{(1)})^4\rho_p^2(q_{p1}^2 - q_{p2}^2) - q_{p1}^4q_{p2}^2((S_{32} + C_{p44})C_{p11} + 2C_{p15}C_{p46}) + 2q_{p1}^3q_{p2}^3(C_{p35}C_{p66}\\
&- C_{p15}(S_{32} + C_{p44})) + 2q_{p1}q_{p2}^5((S_{32} + C_{p44})C_{p35} + C_{p33}C_{p46}) - 2q_{p1}^5q_{p2}(C_{p11}C_{p46} + C_{p15}C_{p66})\\
&+ q_{p1}^2q_{p2}^4(C_{p33}C_{p66} + 4C_{p35}C_{p46}) - q_{p1}^6C_{p11}C_{p66}) + S_{32}(q_{p2}^6(C_{p33}C_{p55} - C_{p35}^2) + q_{p1}^4q_{p2}^2(C_{p11}C_{p55}\\
&- C_{p15}^2) + q_{p1}^2q_{p2}^4(C_{p11}C_{p33} - C_{p13}^2 - 2C_{p13}C_{p55} + 2C_{p15}C_{p35}) + 2q_{p1}^3q_{p2}^3(C_{p11}C_{p35} - C_{p13}(C_{p15}\\
&+ C_{p35})) + 2q_{p1}q_{p2}^5C_{p15}C_{p33} - (c^{(1)})^2\rho_p^2(q_{p1}^2q_{p2}^2(C_{p11} + C_{p55}) - 2q_{p1}q_{p2}^3(C_{p15} + C_{p35}) - q_{p2}^4(C_{p33}\\
&+ C_{p55})) + (c^{(1)})^4\rho_p^2q_{p2}^2) + (c^{(1)})^4\rho_p^2(q_{p1}^2(C_{p11} + C_{p33} + C_{p44} + C_{p55} + C_{p66}) + 2q_{p1}q_{p2}(C_{p15}\\
&+ C_{p35})) + (c^{(1)})^2\rho_p(q_{p1}^2q_{p2}^2(C_{p13}^2 + C_{p55}(2C_{p13} - C_{p44}) - C_{p11}(C_{p33} + C_{p44}) - 2C_{p15}(C_{p35}\\
&+ 2C_{p46}) - 4C_{p35}C_{p46} - C_{p66}(C_{p55} + C_{p33})) + 2q_{p1}^3q_{p2}(C_{p15}(C_{p13} - C_{p66}) - C_{p35}(C_{p11} + C_{p66})\\
&- C_{p46}(C_{p55} + C_{p11})) + 2q_{p1}q_{p2}^3(C_{p35}(C_{p13} - C_{p44}) - C_{p46}(C_{p55} + C_{p33}) - C_{p15}(C_{p33} + C_{p44}))
\end{aligned}
$$

$$+ q_{p1}^4(C_{p15}^2 - C_{p11}(C_{p55} + C_{p66}) - C_{p55}C_{p66}) + q_{p1}^4(C_{p35}^2 - C_{p33}(C_{p44} + C_{p55}) - C_{p44}C_{p55}))$$
$$+ q_{p1}^2 q_{p2}^4(C_{p44}(C_{p11}C_{p33} - C_{p13}^2 - 2C_{p13}C_{p55} + 2C_{p15}C_{p35}) + 4C_{p46}(C_{p15}C_{p33} - C_{p13}C_{p35})$$
$$+ C_{p66}(C_{p33}C_{p55} - C_{p35}^2)) + 2q_{p1}^3 q_{p2}^3(C_{p46}(C_{p11}C_{p33} - C_{p13}^2) + C_{p15}(C_{p33}C_{p66} - C_{p13}C_{p44})$$
$$+ C_{p35}(C_{p11}C_{p44} - C_{p13}C_{p66}) + 2C_{p46}(C_{p15}C_{p35} - C_{p13}C_{p55})) + q_{p1}^6 C_{p66}(C_{p11}C_{p55} - C_{p15}^2)$$
$$+ q_{p2}^6 C_{p44}(C_{p33}C_{p55} - C_{p35}^2) + q_{p1}^4 q_{p2}^2(4C_{p46}(C_{p11}C_{p35} - C_{p13}C_{p15}) + C_{p66}(C_{p11}C_{p33} - C_{p13}^2)$$
$$+ C_{p44}(C_{p11}C_{p55} - C_{p15}^2) + 2C_{p66}(C_{p15}C_{p35} - C_{p13}C_{p55})) + 2q_{p1}^5 q_{p2}(C_{p46}(C_{p11}C_{p55} - C_{p15}^2)$$
$$+ C_{p66}(C_{p11}C_{p35} - C_{p13}C_{p15})) + 2q_{p1}q_{p2}^5(C_{p44}(C_{p15}C_{p33} - C_{p13}C_{p35}) + C_{p46}(C_{p33}C_{p55}$$
$$- C_{p35}^2)) - (c^{(1)})^6\rho_p^3, \tag{A4}$$

where $S_{21} = 0.5(\sigma_{22}^0 - \sigma_{11}^0)$, $S_{31} = 0.5(\sigma_{33}^0 - \sigma_{11}^0)$, and $S_{32} = 0.5(\sigma_{33}^0 - \sigma_{22}^0)$.

Appendix B

The elements of the coefficient matrices $\boldsymbol{T}_{p\mathrm{L}}$ and $\boldsymbol{T}_{p\mathrm{R}}$ in Eq. (18) are

$$T_{p\mathrm{L}}(1,q) = 1, \quad T_{p\mathrm{L}}(2,q) = a_{p2q}^{(1)}, \quad T_{p\mathrm{L}}(3,q) = a_{p3q}^{(1)}, \tag{B1}$$

$$T_{p\mathrm{L}}(4,q) = \frac{\mathrm{i}\omega G_{p1q}^{(1)}}{c^{(1)}}, \quad T_{p\mathrm{L}}(5,q) = \frac{\mathrm{i}\omega G_{p2q}^{(1)}}{c^{(1)}}, \quad T_{p\mathrm{L}}(6,q) = \frac{\mathrm{i}\omega G_{p3q}^{(1)}}{c^{(1)}}, \tag{B2}$$

$$T_{p\mathrm{R}}(1,q) = \exp\Big(\frac{\mathrm{i}\omega\alpha_{pq}d_p}{c^{(1)}}\Big), \quad T_{p\mathrm{R}}(2,q) = a_{p2q}^{(1)}\exp\Big(\frac{\mathrm{i}\omega\alpha_{pq}d_p}{c^{(1)}}\Big), \tag{B3}$$

$$T_{p\mathrm{R}}(3,q) = a_{p3q}^{(1)}\exp\Big(\frac{\mathrm{i}\omega\alpha_{pq}d_p}{c^{(1)}}\Big), \quad T_{p\mathrm{R}}(4,q) = \frac{\mathrm{i}\omega G_{p1q}^{(1)}}{c^{(1)}}\exp\Big(\frac{\mathrm{i}\omega\alpha_{pq}d_p}{c^{(1)}}\Big), \tag{B4}$$

$$T_{p\mathrm{R}}(5,q) = \frac{\mathrm{i}\omega G_{p2q}^{(1)}}{c^{(1)}}\exp\Big(\frac{\mathrm{i}\omega\alpha_{pq}d_p}{c^{(1)}}\Big), \quad T_{p\mathrm{R}}(6,q) = \frac{\mathrm{i}\omega G_{p3q}^{(1)}}{c^{(1)}}\exp\Big(\frac{\mathrm{i}\omega\alpha_{pq}d_p}{c^{(1)}}\Big). \tag{B5}$$

Appendix C

The elements of the coefficient matrices $\boldsymbol{M}_1$, $\boldsymbol{M}_2$, $\boldsymbol{N}_1$, and $\boldsymbol{N}_2$ in Eq. (36) are

$$\boldsymbol{M}_1 = \frac{\mathrm{i}\omega}{c^{(1)}}\begin{pmatrix} G_{p12}^{(1)} & G_{p14}^{(1)} & G_{p16}^{(1)} & 0 & 0 & 0 \\ G_{p22}^{(1)} & G_{p24}^{(1)} & G_{p26}^{(1)} & 0 & 0 & 0 \\ G_{p32}^{(1)} & G_{p34}^{(1)} & G_{p36}^{(1)} & 0 & 0 & 0 \\ 0 & 0 & 0 & G_{p11}^{(1)} & G_{p13}^{(1)} & G_{p15}^{(1)} \\ 0 & 0 & 0 & G_{p21}^{(1)} & G_{p23}^{(1)} & G_{p25}^{(1)} \\ 0 & 0 & 0 & G_{p31}^{(1)} & G_{p33}^{(1)} & G_{p35}^{(1)} \end{pmatrix}, \tag{C1}$$

$$\boldsymbol{M}_2 = \begin{pmatrix} 1 & 1 & 1 & 0 & 0 & 0 \\ a_{p22}^{(1)} & a_{p24}^{(1)} & a_{p26}^{(1)} & 0 & 0 & 0 \\ a_{p32}^{(1)} & a_{p34}^{(1)} & a_{p36}^{(1)} & 0 & 0 & 0 \\ 0 & 0 & 0 & 1 & 1 & 1 \\ 0 & 0 & 0 & a_{p21}^{(1)} & a_{p23}^{(1)} & a_{p25}^{(1)} \\ 0 & 0 & 0 & a_{p31}^{(1)} & a_{p33}^{(1)} & a_{p35}^{(1)} \end{pmatrix}, \tag{C2}$$

$$\boldsymbol{N}_1 = \begin{pmatrix} \frac{\mathrm{i}\omega}{c^{(1)}}G_{p11}^{(1)} & \frac{\mathrm{i}\omega}{c^{(1)}}G_{p21}^{(1)} & \frac{\mathrm{i}\omega}{c^{(1)}}G_{p31}^{(1)} & 0 & 0 & 0 \end{pmatrix}^{\mathrm{T}}, \tag{C3}$$

$$\boldsymbol{N}_2 = (1 \quad a_{p21}^{(1)} \quad a_{p31}^{(1)} \quad 0 \quad 0 \quad 0)^{\mathrm{T}}. \tag{C4}$$